STUDY OF BOOST RECTIFIERS WITH ACTIVE INPUT CURRENT WAVESHAPING

A Thesis submitted
in partial fulfilment of the Requirements
for the degree of

MASTER OF TECHNOLOGY

By

LT. S. K. SRIVASTAVA

To the

DEPARTMENT OF ELECTRICAL ENGINEERING

INDIAN INSTITUTE OF TECHNOLOGY KANPUR

March 1997

EE-1997-M-SRI-STU

CONTENTS

ACKNOWLEDGEMENT

I wish to express my heartfelt reverence and gratitude to Professor S. R. Doradla and Dr. B. G. Fernandes for their able guidance, valuable suggestions and patience during the course of this study.

I sincerely acknowledge the help of Mr. Kishore Chatterjee, Mr. Hemant Agarwal, Mr. Rajneesh, Mr. R. K. Singh and Mr. K. Mahapatra for their help during the course of this study.

The goodwill and support of my friends Capt. R. K. Srivastava, Lt. I. Tandon and Lt. P. P. Sachdev was also a great asset to me during my stay at IIT Kanpur.

Finally, I extend my thanks to Mr. Om Prakash Arora and Mr. R. S. Verma of Power Electronics Lab for their help in providing test equipment.

My sincere thanks to Mr. Yash Pal for devoting time in typing this report.

Lt. S. K. SRIVASTAVA

CERTIFICATE

This is to certify that the work contained in the thesis entitled **'STUDY OF BOOST RECTIFIERS WITH ACTIVE INPUT CURRENT WAVE SHAPING'** by **LT. S. K. Srivastava** has been carried out under our supervision and that this work has not been submitted elsewhere for a degree.

March, 1997

Dr. S. R. Doradla
Professor

Dr. B.G. Fernandes
Asst. Professor

Department of Electrical Engineering
Indian Institute of Technology
Kanpur

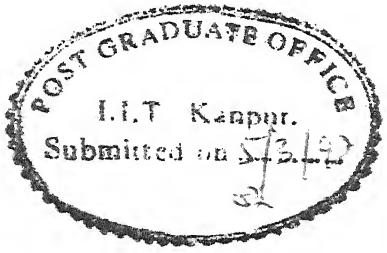

ABSTRACT

Presented in this thesis is the analysis, simulation study and design of single-phase and three-phase rectifier topologies with the boost inductor either on the dc side or on the ac side. The control strategy involves constant frequency, fixed duty ratio and discontinuous current conduction mode of operation in the boost inductor.

The hardware implementation of the three-phase ac-dc boost converts includes a feedback of output voltage control loop to account for fluctuations in the input voltage and load variation. In the simulation of the input current, harmonics upto the harmonic nine have been considered. The total harmonic distortion is found to be less than 4% and the supply power factor is around 0.97.

LIST OF TABLES

LIST OF SYMBOLS

E_a	Phase voltage
i_a	Phase current
e_{ab}, e_{ac}, e_{bc}	Line to line voltage
V_{dc}	dc output voltage
i_L	Inductor current
L_d, L_s, L_b	Inductors
C_f, C_d, C_s	Capacitors
S_1, S_2, SW	Switch
D_1 - D_6	Diodes of Bridge rectifier
D_b	Boost Diode
F_s	Switching frequency
F_L	Line frequency
R	Load
r_e	Effective Series Resistance of Inductor
i_{c_k}	Capacitor C_d current
I_{dc}	Load current
I_{Lk}(avg)	Average boost inductor current over k^{th} switching period
D	Duty ratio
D_1T_s	Instant when inductor current goes to zero
ω	Angular Line Frequency
ΔV_{dc}	Ripple in output voltage
α	Input displacement angle
β	Extinction angle

CHAPTER ONE

INTRODUCTION

1.1 General

The rapid development of increased power level and switching frequency of power semiconductor devices have brought about continuous advancement of power electronics technology leading to perceptible changes in static power converter system. These power converters can perform as power conditioners and uninterruptible power supplies. These are widely used in computers, controlling important processes, medical and communication equipments. However, the power electronic converters inject harmonics into the utility grid causing input supply voltage waveform distortion. It is well known that the phase controlled ac-dc converters cause notches in the utility voltage waveform. At large phase delay angles, the displacement angle also decreases resulting in poor supply power factor.

In most of power electronic equipments such as uninterruptible power supplies (UPS), inverters etc., power conversion takes place using single-phase or three-phase rectifiers. These rectifiers have the following disadvantages :

(i) Pulsed input current which is rich in harmonics

(ii) Due to finite source inductance, voltage waveform distortion at source terminals of converters.

(iii) Low power factor

(iv) High ripple in output dc voltage

Inspite of the diode rectifier have the above mentioned drawbacks, the diode rectifiers are extensively used with input filters [1]-[3], [7]. This improves the input current waveform and power factor. However, filter at line frequency are bulky and, therefore, they are seldom used where weight and size of equipment is of main consideration. Also, a number of national and international agencies have been considering limits on harmonic current injection to maintain good quality of power. Hence, there is a need for high quality rectifiers that present high power factor load to the ac power system and draw line current of low harmonic content.

Therefore, power electronic equipment designers have given a great emphasis to active current waveshaping techniques. The advantages associated with these circuits are :

(i) Improved input current waveform.

(ii) Approximately unity power factor operation.

(iii) Reduction in the size of filter components.

(iv) Reduction in ripple in the output voltage.

(v) Simplicity of control circuitry.

1.2 Outline of thesis

The various active current wave shaping techniques have been developed to improve the input supply power factor of single phase and three phase uncontrolled rectifier. A detailed study of fixed frequency, constant duty ratio technique of active current wave shaping employed to single-phase and three-phase boost rectifiers as shown in Fig. 1.1 - 1.4 have been done. The chapter wise summary is

presented below.

Presented in chapter two is the various techniques of passive and active current wave shaping to improve the power factor. The limitation of these techniques and their suitability in various field is also dealt briefly.

Chapter three and four deal with analysis and parameter calculation for active current wave shaping technique, employed to single-phase and three phase topology respectively. The various factors influencing the component selection has also been listed.

In chapter five the analysis of simulated result has been presented the various plots, graphs and tables in support of these argument have also been attached.

A prototype model of three phase boost rectifier topology has been designed and tested in lab. The hard ware implementation and result obtained in lab are presented in Chapter six.

The conclusion and further improvement and possibility of extending the work has been presented in Chapter seven.

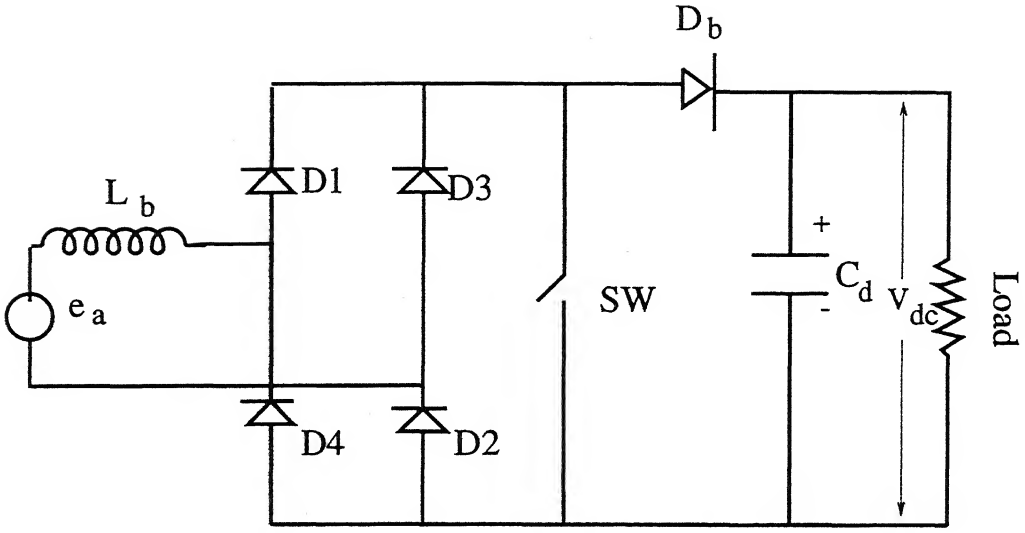

Fig 1.1 Single phase-boost rectifier with boost inductor on ac side

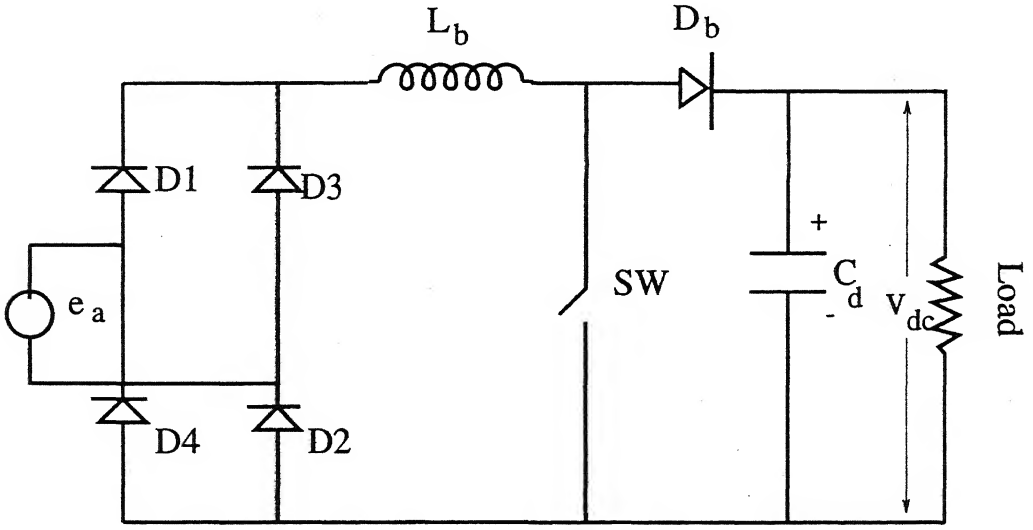

Fig 1.2 Single-phase boost rectifier with boost inductor on dc side

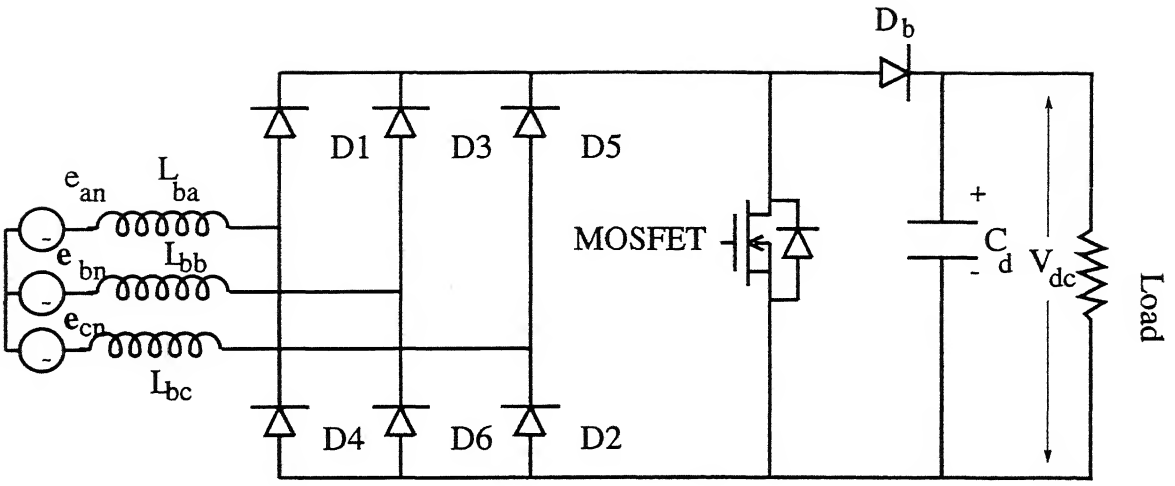

Fig 1.3 Three-phase boost rectifier with boost inductor on ac side

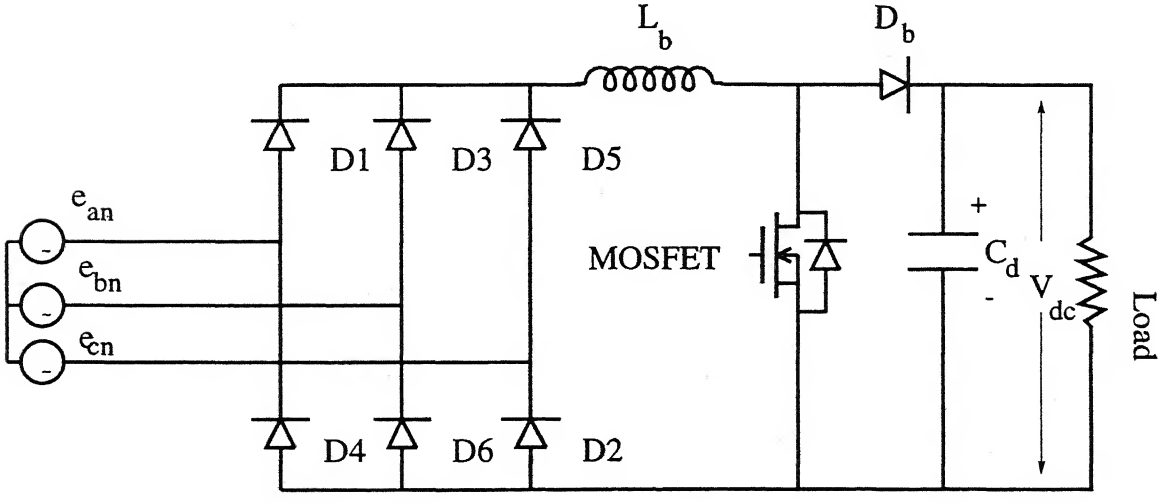

Fig 1.4 Three-phase boost rectifier with boost inductor on dc side

CHAPTER TWO

LITERATURE REVIEW

2.1 INTRODUCTION

The low power factor and high harmonic line currents generated by controlled and uncontrolled rectifiers can lead to voltage distortion, increased losses in distribution system conductors, transformers and shunt capacitors, increased neutral harmonic currents and excitation of system resonance. Therefore, there is a need for low cost, reduced size rectifiers which draws nearly sinusoidal current from the utility. In this chapter the review of ac to dc power converters with passsive and active current waveshaping techniques as reported in literature is presented.

2.2 CONVENTIONAL AC TO DC UNCONTROLLED CONVERTER [1],[7],[17]

AC to DC power conversion is done by single-phase and three-phase uncontrolled rectifiers for low power and for medium to high power respectively. Generally L-C filter is used at the output to reduce the ripple in the output voltage. The equivalent circuit of rectifiers with L-C filter along with output voltage and current waveforms is shown in Fig. 2.1.

If V_{dc} is less than E_m, one pair of diodes start conducting from α which is given by

$$V_{dc} = E_m \sin \alpha \tag{2.1}$$

and the current i_L goes to zero at $\omega t = \beta$.

It is clear from eqn. (2.1) that as V_{dc} approaches E_m, angle α, approaches $\pi/2$. The harmonic content in the input supply current is high. This results in reduction in the input power factor and efficiency. In order to improve the input power factor, a large value of filter inductor (L_d) is required. The output voltage control, however, is not possible with this uncontrolled bridge circuit.

2.3 PASSIVE CURRENT WAVESHAPING TECHNIQUES

In order to improve the supply current waveform, passive current waveshaping techniques are used. Fig. 2.2 shows the use of an input filter inductor L_s for improvement of supply power factor. The performance of the converter of Fig. 2.2 is well reported [7], [16], [18]. If the input filter inductance is very low, the supply current waveform is discontinuous which becomes pulse shaged. This increases the third harmonic component in the input supply current. Though the power factor improves with an increase in L_s, it is not economical.

Another method to improve the supply current waveform is to connect a filter capacitor across the supply as is shown in Fig. 2.3. The corresponding efficiency and power factor is insignificant. A seires resonant filter along with an ac to dc uncontrolled rectifier converter is shown in Fig. 2.4. The quality factor formed by the load and the characteristic impedance of the series resonant circuit together determine the input power factor. The disadvantages of a series resonant input filter are that the reactive elements are of large size and high rms currents flow in the output filter capacitor C_d and input series capacitor C_s. This technique is not

economical for normal supply frequencies of 50 and 60 Hz. However, this topology is generally used in high supply frequency applications as in space platforms [6]. Here, a bandpass filter of series resonant type, whose center frequency is the same as that of supply frequency is connected between the supply and the converter. The quality factor 'Q' of the filter determines its bandwidth which in turn determines the harmonic content of the input supply current. A narrow bandwidth results in less harmonic content and the power factor is close to unity.

The size of the reactive elements of a series resonant filter reduces to some extent by using an input parallel resonant filter [16] which is shown in Fig. 2.5. There is a significant increase in power factor and a decrease in the input current stresses on the reactive elements. Thus, the Voltamper (VA) rating of the reactive components is small.

Though the passive current waveshaping techniques are simple, easy to implement and reliable, they have the following disadvantages :

(1) Large size of the reactive elements.

(2) High rms currents in input/output filter capacitor.

(3) Improved power factor in a restricted range at rated load.

Due to these disadvantages, the passive current wave-shaping techniques are found to be uneconomical and unattractive for certain applications. Active current waveshaping technique are considered in recent times.

2.4 ACTIVE CURRENT WAVESHAPING TECHNIQUE [7]-[14]

With the advent of high power switching devices, such as Power MOSFETs, Power Transistors and IGBTs, active waveshaping of input line current is made possible.

The ac to dc uncontrolled converters employing active waveshaping technique have the following advantages :

(1) Very small lower order harmonic components in input current.

(2) The predominant second harmonic ripple in the output is very small. This results in reduced size of the filter capacitor.

(3) Close to unity power factor operation over a wide operating region with sinusoidal input current.

(4) Ease of applying closed-loop control for load variation.

(5) High efficiency.

(6) Light weight and reduced size of filters due to high switching frequency.

2.4.1 Single-phase switch mode boost reftifier [1],[7]-[8]-[12]

Single-phase switch mode boost rectifier is shown in Fig. 2.6. The switch SW is operated at a high frequency. When the switch is switched on, the current in the boost inductor L_b increases, which is proportional to instantaneous input voltage. The output capacitor C_d supplies the load current during the period when the switch is conducting. When the switch is opened the energy stored in L_b is transferred to the load and the output filter capacitor through the boost diode. The various active current waveshaping techniques as reported in the literature are briefly presented below.

(1) Hysteresis current control with constant window [7]. In this control scheme, a sine reference current of desired magnitude in phase with supply voltage is generated. The inductor current is forced to track the sine reference wave within the desired hysteresis band. The reference current and the actual inductor current waveforms are shown in Fig. 2.7.

(2) Fig. 2.8 shows the modified hysteresis control scheme. In this scheme, the hysteresis is a fixed percentage of instantaneous value of the current. There is a significant improvement in supply current waveform. A digital controller was used to realize this technique. Though the above mentioned HCC techniques are simple to implement providing fast dynamic response, the gating signals are nonuniform. Also, the switching frequency depends on the magnitude of the load current.

(3) Fig. 2.9 shows the scheme for sinusoidal pulse width modulation [7]. In this scheme the gating signal are generated by comapring a high frequency triangular signal with a rectified sine wave signal synchronized with the supply source through a stepdown transformer. Since the device is switched at high frequency, the low order harmonics are either eliminated or reduced. The harmonics at the switching frequency can be easily filtered by small-sized filters. This results in input power factor close to unity.

(4) Another scheme of active current waveshaping is shown in Fig. 2.10 [11] and different modes of operations are

shown in Fig. 2.11. Mode 1 occurs when the input ac voltage is positive and switches are off. The current flows through diode D_1, capacitor and load, and back through the antiparallel diode of S_2. Mode 2 occurs when the input ac voltage is positive and the switches are gated on. The input current flows through switch S_1 and back through the antiparallel diode of S_2. During this mode, the capacitor supplies the load current. Mode 3 starts when the input ac voltage is negative and the switches are off. The current flows through diode D_2, capacitor and load, and back through the antiparallel diode of S_1. Mode 4 occurs when the input ac voltage is negative and the switches are gated on. The input current flows through switch S_2 and back through the antiparallel diode of S_1. The advantages of this configuration are (i) at any given instant, only two semiconductor devices are conducting (ii) the rms current rating of boost switches, S_1 and S_2 is low.

2.4.2 Three-phase active current waveshaping [9],[10],[13]

In industrial applications where three-phase ac voltages are available, it is preferable to use three-phase rectifier circuits over single-phase rectifier because of their lower ripple content in the waveforms and a high power handling capability. The active current waveshaping techniques for the three-phase rectifier circuits reported in the literature are briefly presented in this section.

(1) Hysterisis control method was also reported for a three-phase ac to dc converter which is realised using

three single-phase ac to dc converters [7],[9]. The circuit configuration is shown in Fig. 2.12. There is a significant improvement in the supply current waveform and the power factor is close to unity. However, it has the following disadvantages.

(i) It requires complicated input synchronization logic.

(ii) Owing to variation in power circuit control parameter among the individual converters, a complete triplen harmonic elimination from the input line current can not be achieved.

(iii) Switching frequency is load dependent.

(2) Another topology for power factor correction, with three wye-connected boost inductors on the ac side was also reported [8]. The boost diode is replaced by another switch S_4. The configuration is shown in Fig. 2.13. During each switching cycle, the switches S_1-S_3 conduct for 0 to DT_s, and S_4 conduct for DT_s to T_s (switching period). At the beginning of each switching cycle S_1-S_3 are turned on and S_4 is turned off. The current in a boost inductor increases linearly and the capacitor C_d supplies the load current. At DT_s, switches S_1-S_3 are turned off and S_4 is turned on. The energy stored in the boost inductors is transferred to the load and C_d through S_4.

The values of boost inductance, switching frequency, input and output voltage are so selected that each boost inductor always operates in the discontinuous mode. The shape of the current through a boost inductor is triangular. The

average of these triangular pulses varies sinusoidally. The high frequency harmonic components which are present in the line current can be filtered by a small passive filter whose size depends on the switching frequency. The scheme is easy to implement.

The detailed analysis and the simulation studies of single-phase and three-phase boost rectifer topologies with fixed switching frequency and constant on time are presented in chapters 3 and 4.

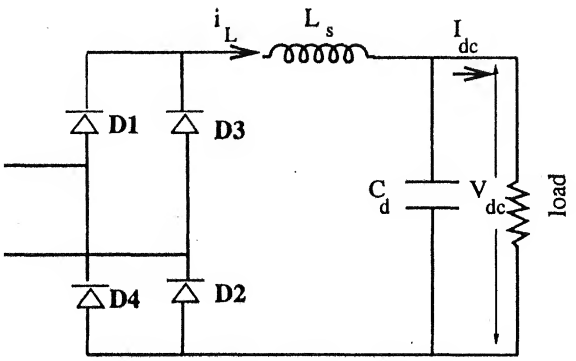

(a) Single-phase Rectifier with L-C filter

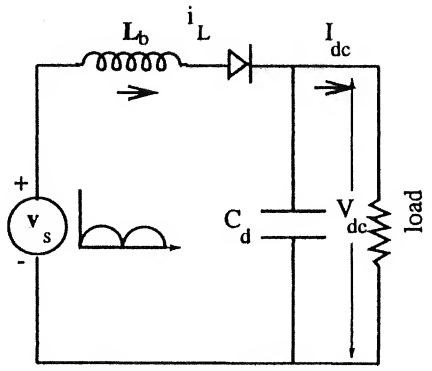

(b) Equivalent circuit

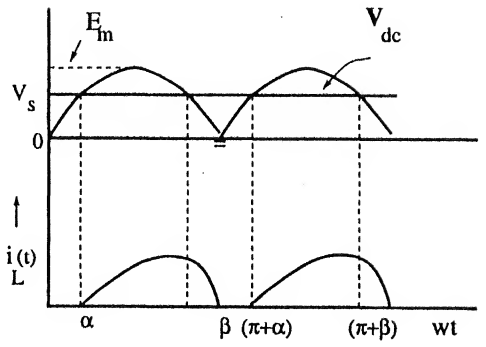

(c) Waveform of equivalent circuit with L -C filter

Fig 2.1 single phase rectifier with L-C filter

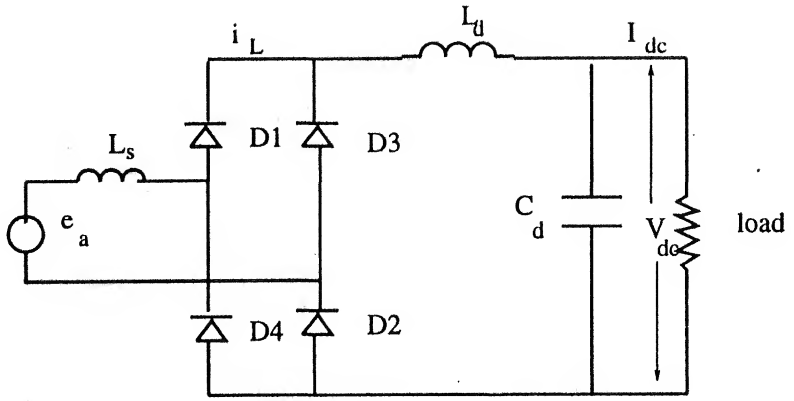

Fig 2.2 Single-phase Rectifier with input filterL s

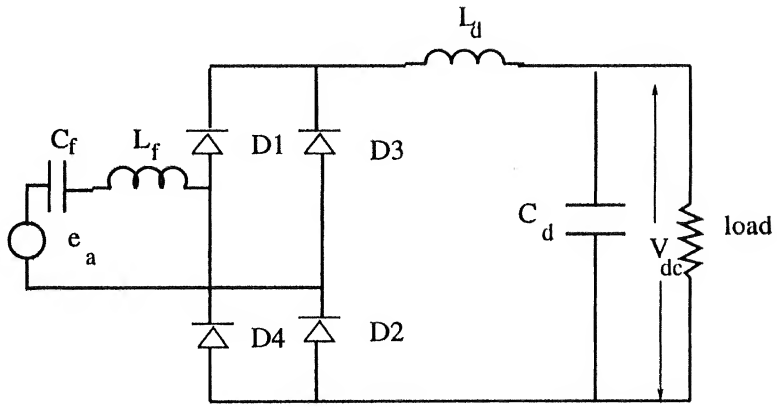

Fig 2.4 Single - phase Rectifier with input series resonent filter

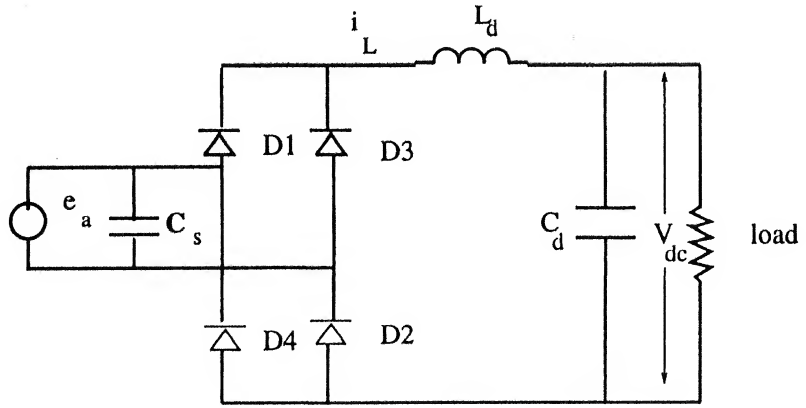

Fig 2.3 Single-phase Rectifier with input filter Cs

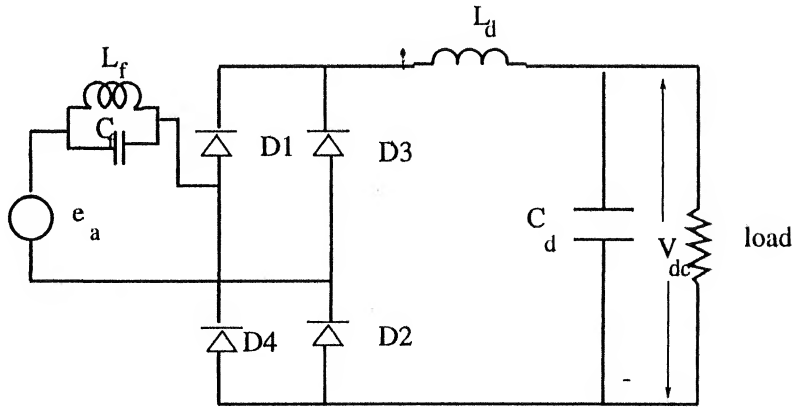

Fig 2.5 Single - phase Rectifier with input parallel resonant filter

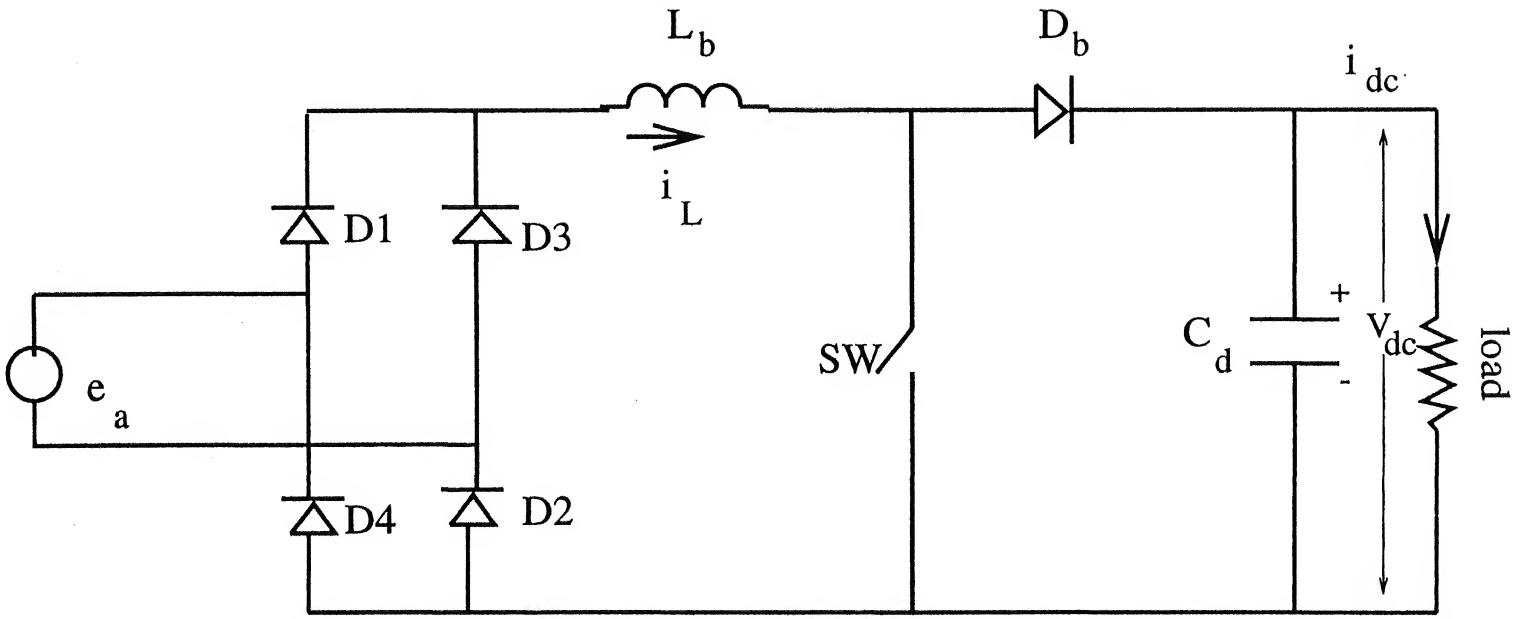

Fig 2.6 Single - phase boost rectifie

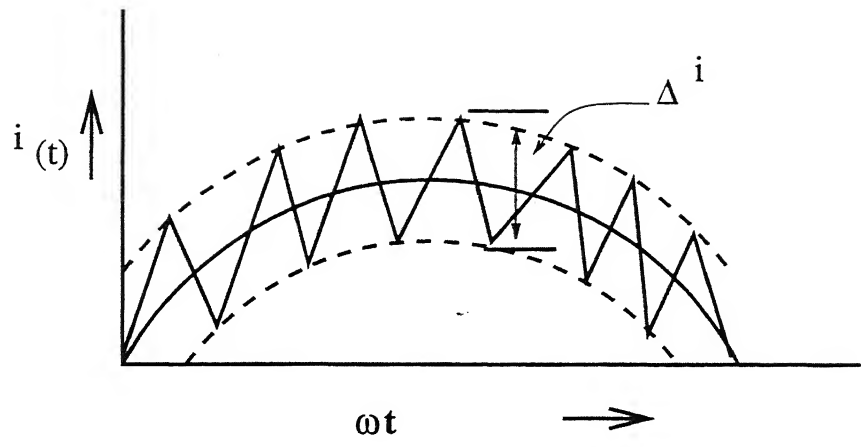

Fig 2.7 Constant Hysterisis band control

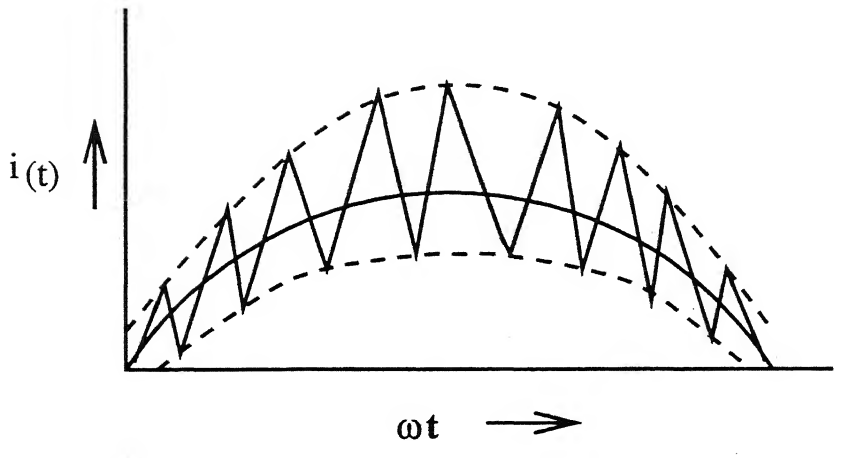

Fig 2.8 Fixed percentage HCC

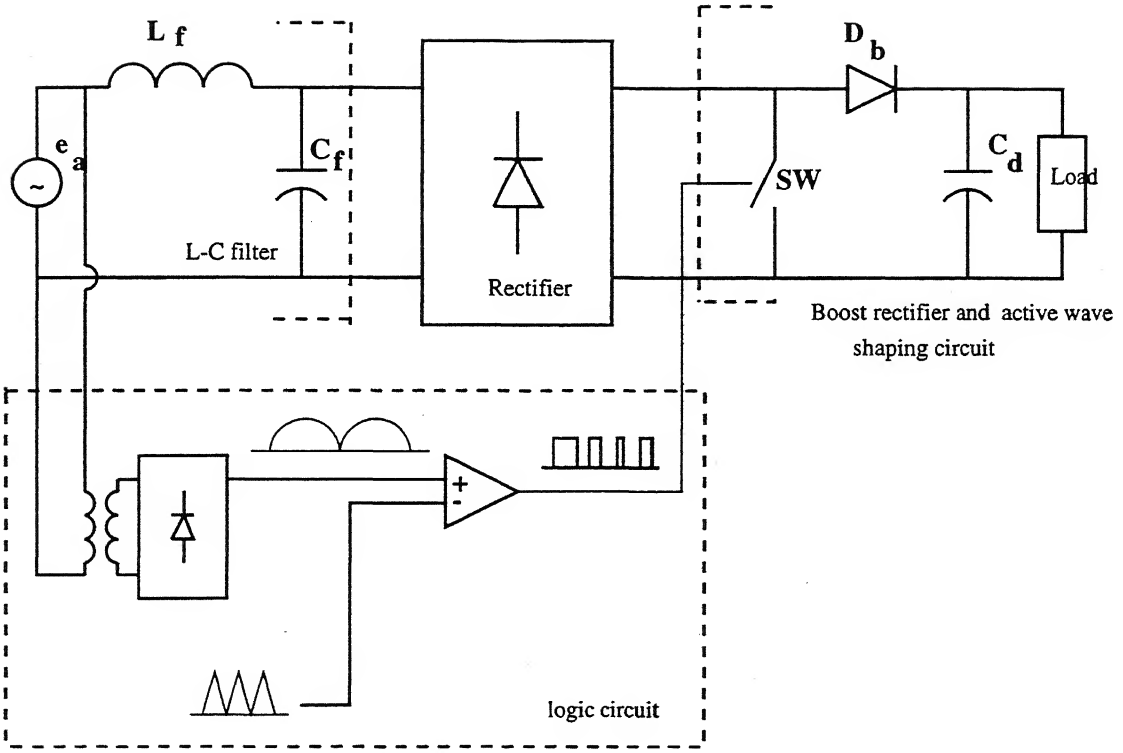

Fig 2.9 Block Diagram of Sinusoidal Pulse Width Modulation

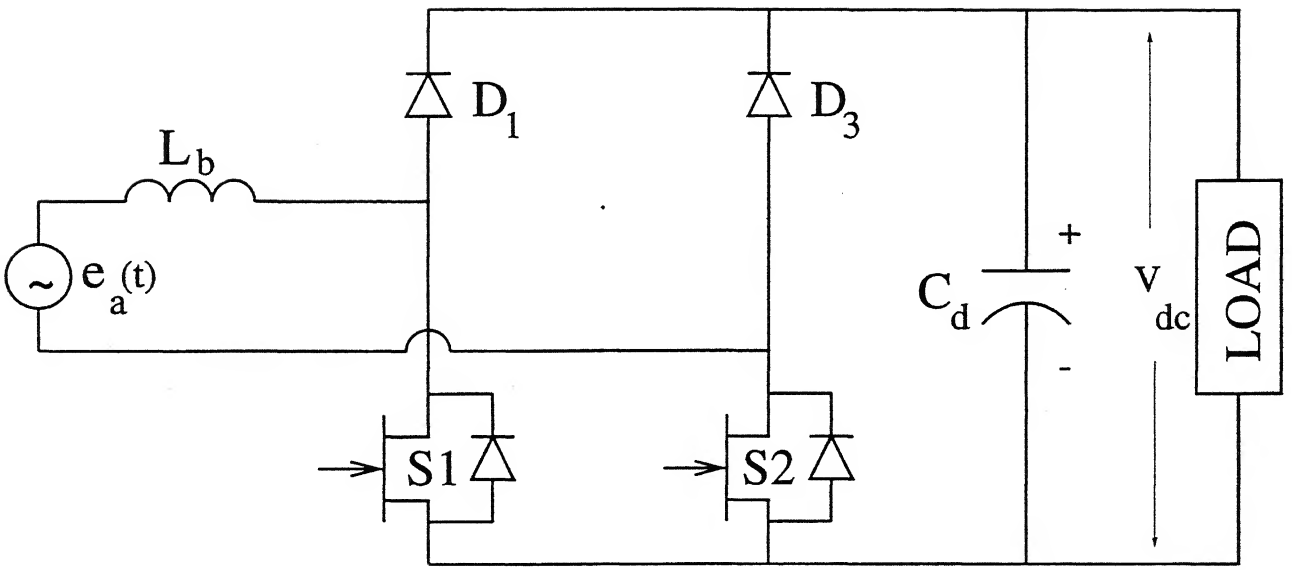

Fig 2.10 Boost rectifier without boost diode

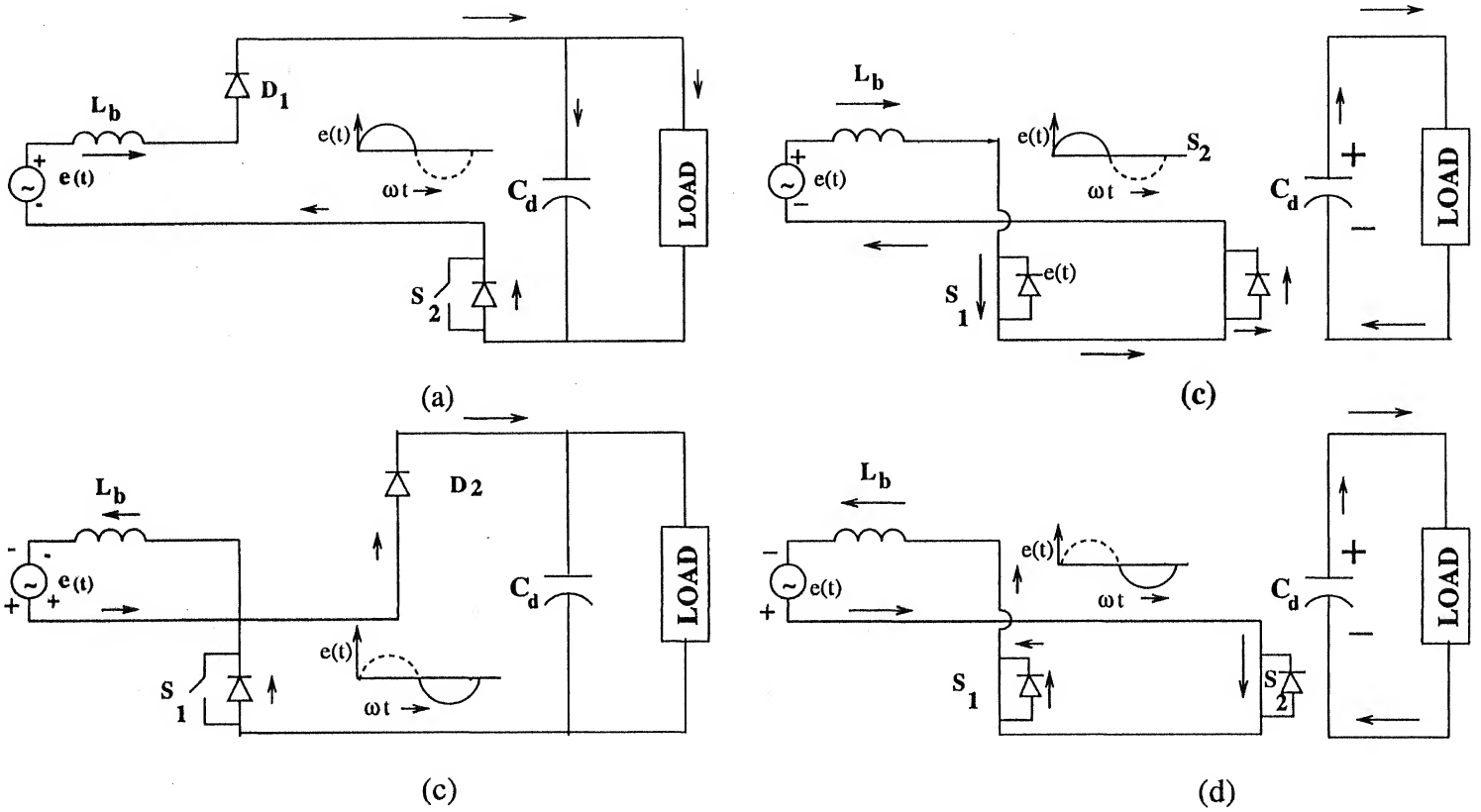

Fig 2.11 Different modes of operation of boost rectifier of Fig 2.10

(a) mode 1 (b) mode 2 (c) mode 3 (d) mode 4

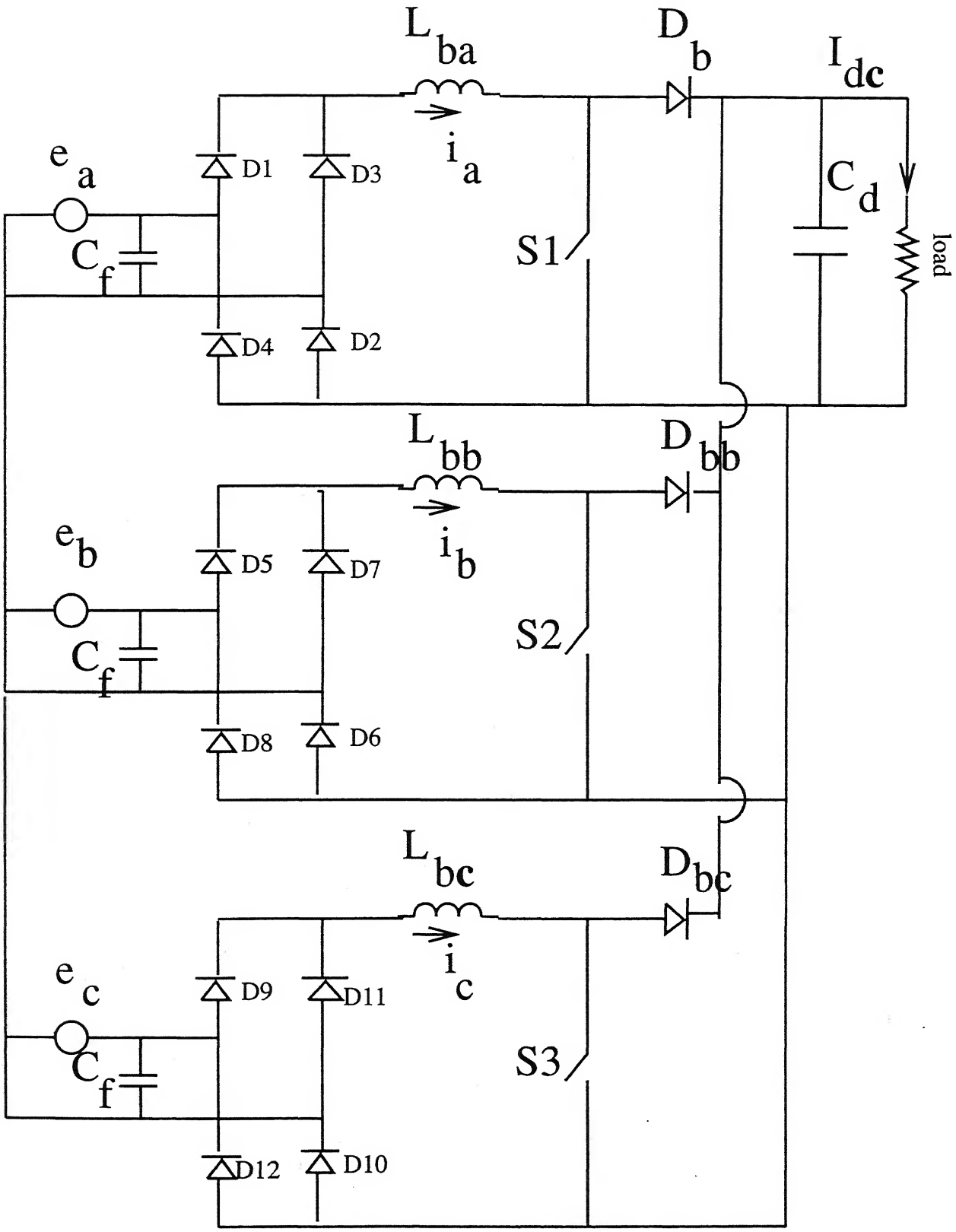

Fig 2 .12 Three - phase boost rectifier configuration

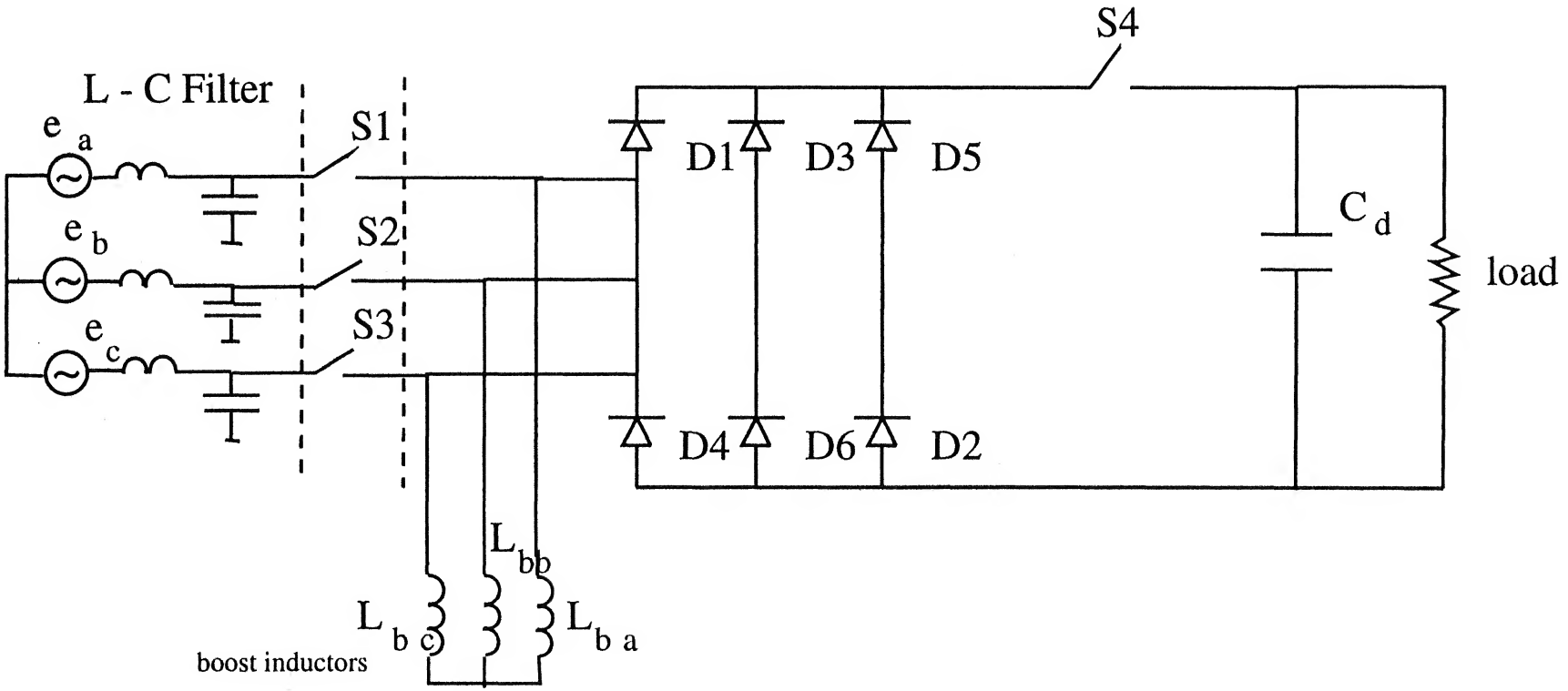

Fig 2.13 Three-phase boost rectifier

CHAPTER THREE

SINGLE-PHASE BOOST RECTIFIER

3.1 INTRODUCTION

Active current waveshaping technique is gaining popularity over passing current waveshaping technique due to its improved harmonic spectrum, lower size and improved power factor. Two basic single-phase unity power factor boost rectifiers are shown in Figs. 3.1 and 3.2. These are the same as described in chapter 1 and 2. By using these circuits, it is possible to shape the input current drawn by the rectifier to be sinusoidal and in phase with the input voltage.

3.2 SINGLE-PHASE BOOST RECTIFIER WITH BOOST INDUCTOR ON AC SIDE

In the configuration of Fig. 3.1, the switching frequency F_s of the switch SW is very high compared to line frequency f_L. During each switching cycle, the switch is closed for DT_s sec. and it is open for $(1-D)T_s$ sec.

The different modes of operation are shown in Fig. 3.3. Mode 1 starts at KT_s where K = 0....n, n is the number of switchings per half cycle ($n = F_s/2F_L$) and it ends at $(K+D)T_s$.

When the switch SW is closed, the boost inductor L_b charges through the diode D_1, switch SW and diode D_2. The boost diode D_b is reverse biased and the output capacitor C_d supplies the load current.

The differential equations governing this mode of

operation are,

$$L_b \cdot \frac{di_L}{dt} + r_e i_L(t) = e_a(t) \qquad (3.1)$$

$$C \frac{dV_{dc}}{dt} = \frac{Vd_{dc}}{R} \qquad (3.2)$$

Mode 2 starts at $t = (K+D)T_s$. Switch SW is turned off. The stored energy in the inductor is transferred to the output capacitor and load. Since the output voltage is higher than the instantaneous source voltage, the inductor current decreases. The equivalent circuit for this mode is shown in Fig. 3.3(b).

The differential equations governing the operation of the circuit during this mode are,

$$\frac{Ldi_L}{dt} + r_e.i_L + V_{dc} = e_a(t) \qquad (3.3)$$

$$i_L = i_C + i_{dc} \qquad (3.4)$$

where i_L and i_C are inductor and capacitor currents respectively and r_e is effective series resistance of inductor. Modes 3 and 4 are similar to modes 1 and 2. The only difference is that the input supply is negative and diodes D_3 and D_4 conduct instead of diodes D_1 and D_2. In this topology the current through inductor is ac and average value of it is zero. The different voltage and current waveforms are shown in Fig. 3.4.

3.3 SINGLE-PHASE TOPOLOGY WITH BOOST INDUCTOR ON DC SIDE

The operation of the circuit shown in Fig. 3.2 is similar to that of, shown in Fig. 3.1. Since the boost inductor is connected in the dc side, the current through it is dc.

An approximate relationship between output and input voltage for boost converter can be obtained from the equivalent circuit where the rectifier is represented by an equivalent dc source which delivers the voltage equal to average voltage of rectifier. The equivalent circuit used for the analysis is shown in Fig. 3.5.

The average output voltage in terms of switching duty ratio is given by

$$V_{dc} = \frac{e_{a(av)}}{(1-D)}$$

3.4.1 Analysis of input current

The following assumptions are made while analysing the converter shown in Fig. 3.1 under steady state.

(1) Switching device and all power diodes are ideal.Forward voltage drop and reverse leakage currents of diodes are negligible.

(2) Boost inductor and output filter capacitor are ideal.

(3) As the switching frequency F_s is very high compared to line frequency F_L, the input supply voltage is assumed to be piecewise linear as shown in Fig. 3.4(e), i.e., its value remains constant during each switching cycle.

(4) Output voltage is ripple free.

The inductor current (boost-inductor) is triangular in shape as shown in Fig. 3.6. For $0\text{-}DT_s$ in each switching cycle it increases linearly when switch is closed and it decreases towards zero when switch is turned off and the boost diode D_b is conducting. It is assumed that during each switching period, the input voltage remains constant and its value is given by,

$$E_a(t_k) = E_m \sin(\omega t + \alpha)$$

where $\alpha = k\omega T_s$, $k = 1...n$ and $n = f_s/2f_L$.

For Mode 1, the relationship between the supply voltage and the inductor current is given by

$$E_a(t_k) = L_b \frac{di_L(t)}{dt} \tag{3.5}$$

at $t = dT_s$, switch is turned off and boost diode starts conducting. The relationship between supply voltage, inductor current and output voltage is given by

$$E_a(t_k) = L_b \frac{di_L(t)}{dt} + V_{dc} \qquad T_{k-1}DT_s < t < T_k \tag{3.6}$$

The peak inductor current during any switching cycle can be obtained from equation (3.5),

$$I_L(t) = \int_{kT_s}^{kT_s+DT_s} \frac{E_a(t_k)}{L_b}\, dt$$

or,

$$I_{2k} \text{ (Peak current)} = \frac{E_a(t_k)}{L_b} DT_s \tag{3.7}$$

When the switch is turned off inductor current starts

decreasing and becomes zero at instant $D_{1k}T_s$ during kth switching cycle. The value of $D_{1k}T_s$ can be obtained by solving equation (3.6)

$$L_b \frac{di_L}{dt} = E_a(t_k) - V_{dc}$$

or

$$I_L(t) = \int_{kT_s+DT_s}^{kT_s+ DT_s+ D_{1k}T_s} \frac{E_a(t_k) - V_{dc}}{L_b} dt + I_2$$

or, $$I_{3k} = \frac{E_a(t_k) - V_{dc}}{L_b} (D_1T_s) + \frac{E_a(t_k)}{L_b} DT_s$$

Since inductor current is discontinuous, $I_{3k} = 0$.

or, $$d_{1k} = \frac{E_a(t_k).D}{V_{dc}-E_a(t_k)} \qquad (3.8)$$

The average inductor current for a switching period (T_s) can be obtained by equating the area of triangle over one switching period with the area of average current over the same period.

If $I_{Lk}(av)$ is average value of the boost inductor current over k^{th} switching cycle, then its value can be obtained as,

$$I_{Lk}(av)T_s = \frac{1}{2} I_{2k}(D + D_{1k}) T_s$$

or, $$I_{Lk}(av) = \frac{1}{2} I_{2k}(D + D_{1k}) \qquad (3.9)$$

Substituting the value of I_{2k} and D_{1k} from (3.8) into (3.9).

$$I_{Lk}(av) = \frac{1}{2} \frac{E_a(t_k)}{L_b} DT_s \left\{ D + \frac{E_a(t_k)D}{V_{dc}-E_a(t_k)} \right\}$$

$$= \frac{1}{2} \frac{E_a(t_k)}{L_b} D^2T_s \left\{ \frac{V_{dc}}{V_{dc}-E_a(t_k)} \right\} \qquad (3.10)$$

If a high frequency filter is connected between the boost inductor and the input source, the average current drawn from the source will vary sinusoidally at line frequency and all high frequency harmonics will be filtered out. The current drawn from the source will be in phase with the input voltage.

3.4.2 Analysis of output voltage

The output voltage can be obtained by assuming that the ripple over half line cycle is zero. Then, the average of boost diode current flows through the load and all the ripple is passed through the output filter capacitor.

The output current calculation can be done graphically from the boost diode current which is shown in Fig. 3.4(c). The average value of boost diode current over half cycle can be obtained by summing the area of individual triangle over o-π period and equating it to the load current which is assumed to be constant and equal to I_{dc}.

The area of k^{th} triangle is given by,

$$\Delta = \frac{1}{2} I_{2k} . D_{1k} T_s \tag{3.11}$$

There are 'n' such triangle over each half cycle period. The average value of boost diode current is given by,

$$I_{dc} . nT_s = \sum_{k=1}^{n} \frac{1}{2} I_{2k} D_{1k} T_s \tag{3.12}$$

Substituting the value I_{2k} and D_{1k} from equations (3.7) and (3.8) into (3.12) and after necessary simplification yields

$$I_{dc} = \frac{D^2 T_s}{2nL_b} \sum_{k=1}^{n} \left\{ \frac{E_a(t_k)}{V_{dc} - E_a(t_k)} \right\} \tag{3.13}$$

3.4.3 Output voltage ripple calculation

The riple in output can be calculated graphically from Fig. 3.4(c),

$$\Delta V_{dc}(t) = \frac{1}{C_d}\int_0^t i_{ck}(t)\,dt\,, \qquad t \in [0,\ \pi/\omega] \tag{3.14}$$

From the graphical interpretation of integral,

$$\Delta V_{dc}(nT_s) = \frac{1}{C_d}\sum_{k=1}^{n}\frac{1}{2} I_{2k} d_{1k} T_s - \frac{nI_{dc}T_s}{C_d} \tag{3.15}$$

$$\Delta V_{dc} = \frac{D^2T_s^2}{2LC_d}\sum_{k=1}^{n}\frac{E_a^2(t_k)^2}{V_{dc} - E_a(t_k)} - \frac{nI_{dc}T_s}{C_d} \tag{3.16}$$

However, Ned Mohan et al. [1] have suggested a simple method to determine the ripple content in the output voltage. It is assumed that the converter is ideal and the switching frequency is very high. Therefore, the size of the boost inductor will be negligibly small. Equating instantenous input power and output power, we get

$$p_{in}(t) = E_m \sin \omega t \,.\, I_m \sin \omega t = e_a.i_a - e_a.i_a \cos 2\omega t \tag{3.17}$$

From (3.4),

$$i_{Lk}(t) = I_{dc} + i_c(t) \tag{3.18}$$

where average value of $i_{L_k}(t) = I_{L_k}(av) = I_{dc} = \dfrac{e_a i_a}{V_{dc}}$ (3.19)

and the current through capacitor is

$$i_c(t) = -\frac{e_a i_a}{V_{dc}} \,.\, \cos 2\omega t = - I_{dc} \cos 2\omega t \tag{3.20}$$

The ripple in capacitor voltage is given by,

$$\Delta v_{dc} = \frac{1}{C_d} \int i_c \, dt \simeq \frac{I_{dc}}{2\omega C_d} \sin 2\omega t \qquad (3.21)$$

From (3.21) it can be inferred that the output voltage will have ripple which varies sinusoidally at twice the supply frequency. Depending upon the permissible limit of ripple in output voltage, the value of C_d is given by

$$C_d \geq \frac{I_{dc}}{2\omega \, \Delta \, V_{dc}} \qquad (3.22)$$

Equation (3.22) gives an approximate value of output filter size. However, for more accurate design eqn. (3.16) could be used.

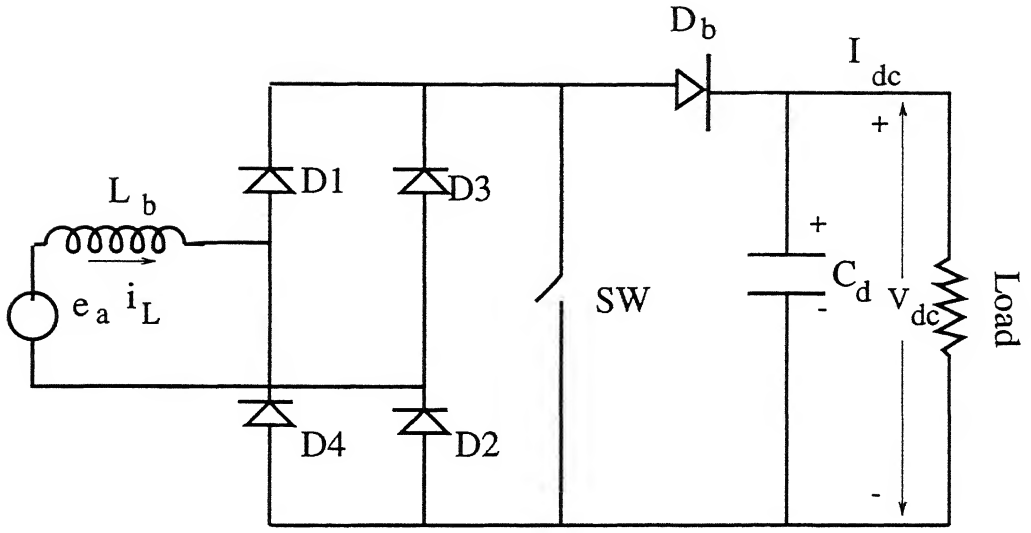

Fig 3.1 Single phase-boost rectifier with boost inductor on ac side

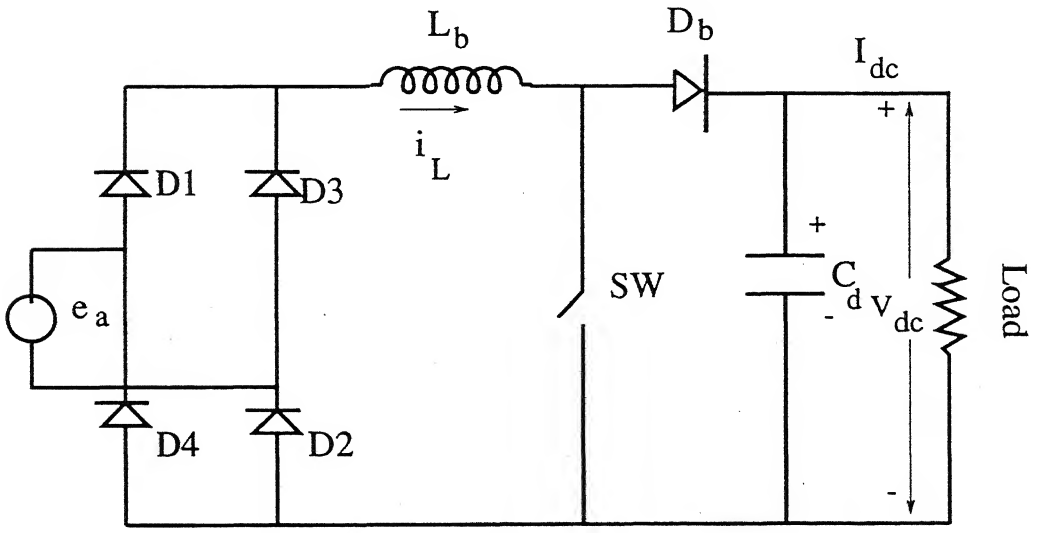

Fig 3.2 Single-phase boost rectifier withboost inductor on dc side

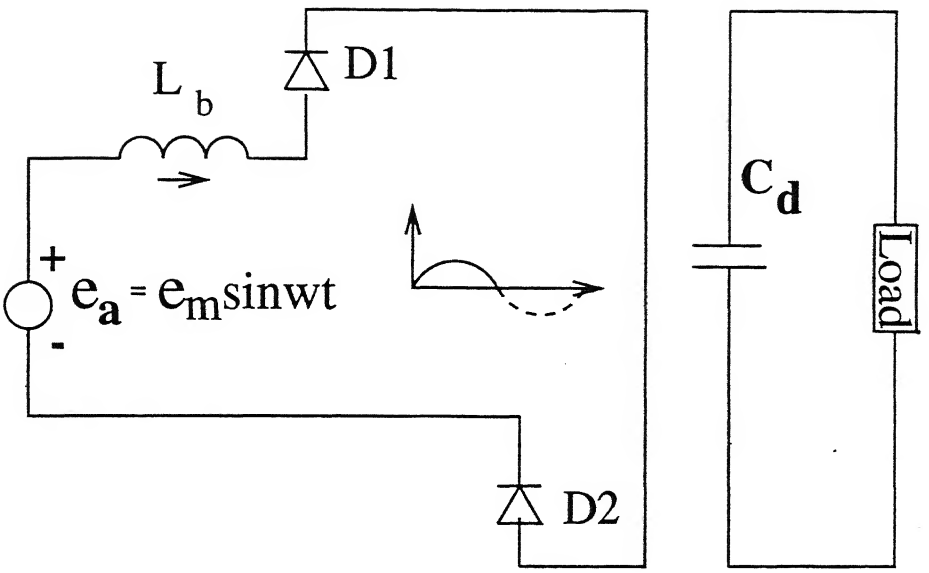

(a)

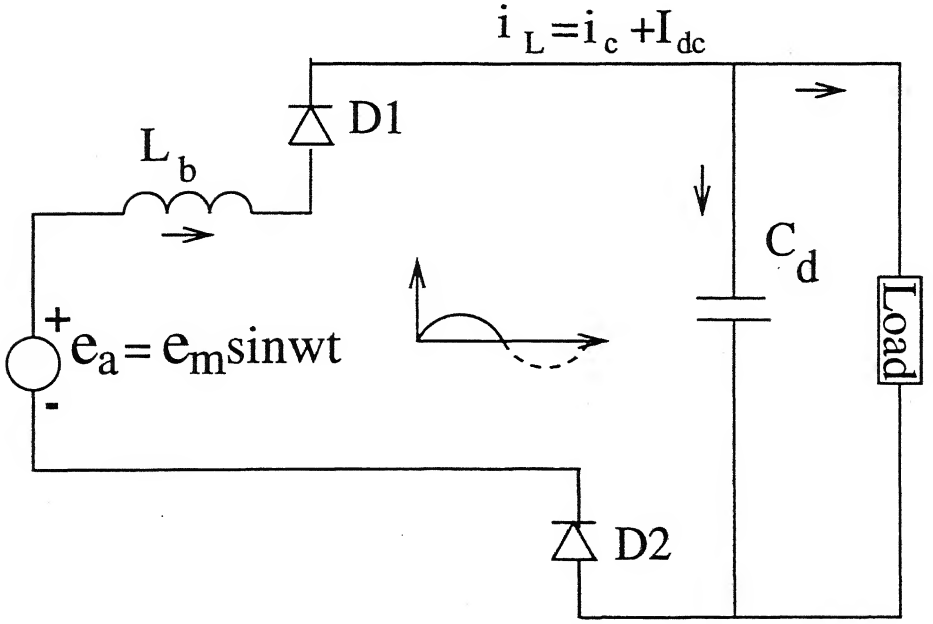

(b)

Fig 3.3 Equivalent circuit for different modes of boost rectifier

of Fig of 3.2 (a) mode 1 (b) mode 2

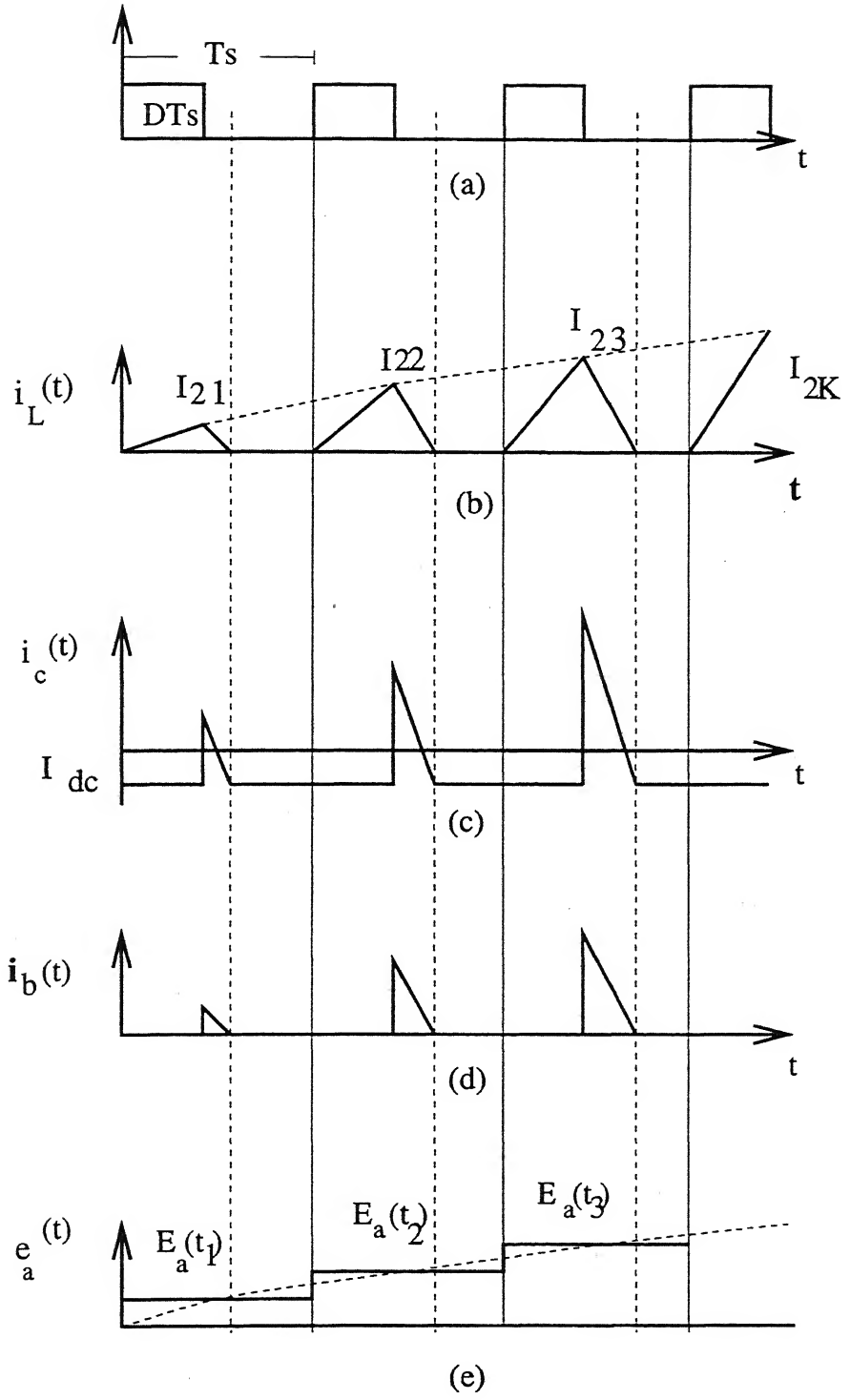

Fig 3.4 Waveforms of gating signals and some corresponding voltage and current waveforms

(a) Gating signals (b) Boost inductor current

(c) Capacitor C_d current (d) Boost diode current

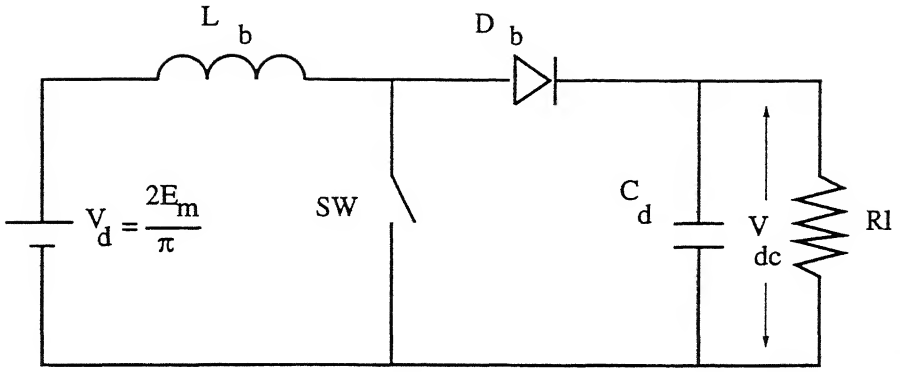

Fig 3.5 Equivalent circuit of boost rectifier of Fig 3.2

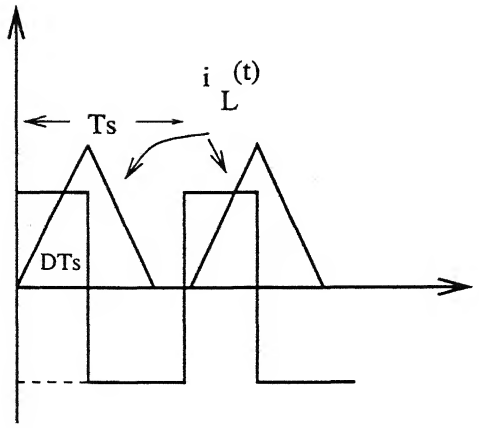

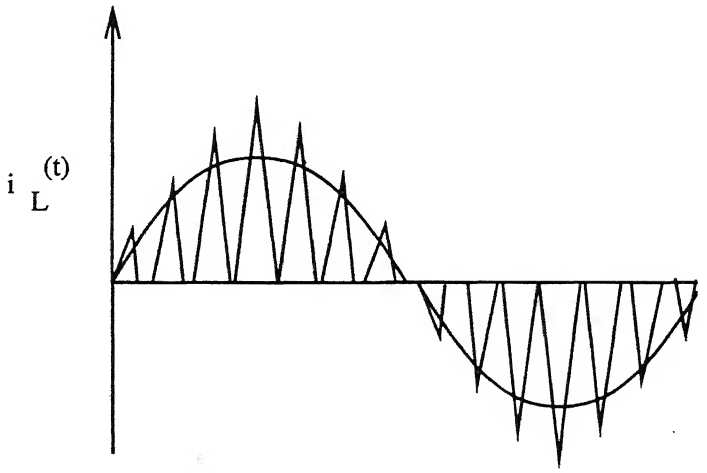

ɜ 3.6 Magnified boost inductor current

Fig 3.7 Waveform of boost inductor current of l

CHAPTER FOUR

THREE-PHASE SWITCH MODE BOOST RECTIFIER

4.1 INTRODUCTION

Generally three-phase rectifiers are used in high power conversion. Fig. 4.1 and 4.2 shows two topologies of boost rectifier. In Fig. 4.1 the boost inductor is placed on the dc side whereas in Fig. 4.2 three boost inductors are placed on ac side. The principle of operation and detailed analysis of these converters is presented in this chapter.

4.2 PRINCIPLE OF OPERATION OF BOOST RECTIFIER WITH INDUCTOR ON DC SIDE

The operation of the circuit shown in Fig. 4.1 can be viewed such that the boost inductor and load are supplied by a three-phase uncontrolled rectifier. Two diodes, one in the upper group (D_1, D_3, D_5) and another in the lower group (D_4, D_6, D_2) each conduct for a duration of 120°in each line cycle and there are six intervals each of 60° with the diodes (D_1D_2, D_2D_3, D_3D_4, D_4D_5, D_5D_6) conducting.

The six intervals depend on the instantaneous values of input line to line voltages. The sequence of diodes conduction is D_1D_2, D_2D_3, D_3D_4, D_4D_5, D_5D_6 and D_6D_1. For analysis of this circuit, it is assumed that the switching frequency of the switch is 6n times that of line frequency. Therefore, during

each 60° interval, the switch SW is switched on n times.

or $$n = \frac{F_s}{6F_L} \tag{4.1}$$

where F_L and F_s represent line and switching frequency.

During each switching period there are two modes (i) when SW is closed, energy is stored in the boost inductor, (ii) when SW is opened, the stored energy in the boost inductor is transferred to the output capacitor and load. The equivalent circuits for these modes are shown in Fig. 4.3.

When the switch is closed the current in the boost inductor increases linearly and the load current is supplied by the output filter capacitor. The differential equations governing this mode are

$$e_{ab} = E_m \sin(\omega t + \pi/3) = L_b \cdot \frac{di_L}{dt} \tag{4.2}$$

$$C_d \frac{V_{dc}}{dt} = \frac{V_{dc}}{R} \quad ; \quad T_k < t < T_k + DT_s \tag{4.3}$$

Where T_k is the k^{th} switching period.

At $t = T_k + DT_s$ the switch is opened. The inductor current flows through the boost diode thereby transferring the energy stored in the inductor to load. The differential equations governing this mode are,

$$e_{ab} = E_m \sin(\omega t + \pi/3) = L_b \cdot \frac{di_L}{dt} + V_{dc} \tag{4.4}$$

$$i_L(t) = C_d \frac{dV_{dc}}{dt} + \frac{V_{dc}}{R} \tag{4.5}$$

4.2.1 Expression for inductor current and output voltage

In order to derive an expression for inductor current, it is assumed that line to line voltages (e_{ab}, e_{ac}, etc) remains constant during switching period and its value is given by

$$E_{ab}\ (t_k) = e_{ab} \sin \alpha$$

where $\alpha = (\pi/3 + KT_s\omega)$ $\qquad$ K = 0 to n.

Also, all the switching devices and passive elements are ideal and the output voltage is assumed to be ripple free.

When the switch is switched on, the inductor current increases linearly and its value during K^{th} cycle is given by

$$i_L(t) = \frac{e_{ab}(t_k)}{L_b}\, t \qquad (4.5)$$

where $e_{ab}(t_k) = E_{ab}(t_k)$ for Kth switching cycle.

At the end of DT_s, the peak current in the inductor is given by,

$$I_{2k} = \frac{E_{ab}(t_k)}{L_b}\, DT_s \qquad (4.6)$$

When the boost switch SW is switched off, the inductor current starts reducing. The expression for the inductor current is

$$i_L(t) = \frac{E_{ab}(t_k) - V_{dc}}{L_b}\, t + I_{2k} \qquad (K+D)T_s < t < (K+D+D_1)T_s \qquad (4.7)$$

The current in the inductor (L_b) becomes zero before the switch is turned on again. This instant of time when the inductor current is zero is given by $(K+D+D_1)T_s$. From (4.7),

$$D_{1k} = \frac{E_{ab}(t_k)D}{\{V_{dc}-E_{ab}(t_k)\}} \qquad (4.8)$$

4.2.2 Output voltage V_{dc} calculation

The computation of output voltage V_{dc} over 1/6th period of supply frequency can be done graphically from Fig. 4.4(d). It is assumed that the average value of the boost diode current flows through the load while the ripple current flows through the capacitor.

Therefore, from equation (4.5)

$$C_d \frac{dV_{dc}}{dt} = i_{Lk}(avg) - \frac{V_{dc}}{R} \qquad (4$$

where $i_{Lk}(avg)$ is average value of the current in the boost diode which can be calculated graphically from Fig. 4.4(d) and it is equal to

$$i_{Lk}(avg) = \frac{1}{T_L/6} \sum_{k=1}^{n} \frac{I_{2k}}{2} D_{1k}T_s$$

$$i_{Lk}(avg) = \frac{3\omega}{\pi} \sum_{k=1}^{n} \frac{I_{2k}}{2} D_{1k}T_s \qquad (4.10)$$

where $T_L = 2\pi/w$

The values of $i_{Lk}(avg)$ and D_{1k} are substituted in equation (4.9). The expression for the output voltage is given by

$$V_{dc} = \frac{3\omega}{\pi} D^2T_s^2 \sum_{k=1}^{n} \frac{E_{ab}^2(t_k)}{V_{dc}-E_{ab}(t_k)} R \qquad (4.11)$$

4.3 THREE-PHASE SWITCH MODE BOOST RECTIFIER WITH INDUCTORS ON AC SIDE

Fig. 4.2 shows the circuit of three-phase boost rectifier with inductors on ac side. The principle of operation of the circuit is same as that with inductor on dc side. The currents in boost inductors L_{ba}, L_{bb} and L_{bc} increase at a rate which is proportional to the respective phase voltages, when switch SW is closed. They decrease to zero when the switch is turned off. Unlike in a normal three-phase rectifier the diodes in this circuit conduct for 180°. Thus, the fundamental component of the current in a phase is in phase with the corresponding phase voltage.

For analysis of the circuit shown in Fig. 4.2, it is assumed that the three-phase supply voltages are balanced. The supply frequency 50Hz is much lower when compared to the switching frequency. At any instant of time three diodes of the bridge are conducting and each combination conduct for 60°. Therefore, there are six intervals during each line cycle. If the 3-phase voltages are

$$e_a = E_m.\sin\omega t \tag{4.12}$$

$$e_b = E_m.\sin(\omega t - 2\pi/3) \tag{4.13}$$

$$e_c = E_m.\sin(\omega t - 4\pi/3) \tag{4.14}$$

Then, the six diode combinations are

Interval	Diodes Conducting
$0 - \frac{\pi}{3}$	$D_1\ D_5\ D_6$
$\frac{\pi}{3} - \frac{2\pi}{3}$	$D_1\ D_2\ D_6$
$\frac{2\pi}{3} - \pi$	$D_1\ D_2\ D_3$
$\pi - \frac{4\pi}{4}$	$D_4\ D_2\ D_3$
$\frac{4\pi}{3} - \frac{5\pi}{3}$	$D_4\ D_5\ D_3$
$\frac{5\pi}{3} - 2\pi$	$D_4\ D_5\ D_6$

When the switch SW is closed the current in each boost inductor increases linearly from zero at a rate proportinal to the respective phase voltage. The peak value of the current is given by

$$i_{L\phi K} = \frac{DT_s}{L_b} e_{\phi n} \tag{4.15}$$

where ϕ indicates phase a, b, or c

When the switch is turned off the inductor current flows through the boost diode. The stored energy in the inductors is transferred to the output and the current decreases. The rate of decrease of the current in the inductor depends upon the output voltage V_{dc} and the input phase voltage $V_{\phi n}$. The inductor current becomes zero before the switch SW is turned on again.

The single phase equivalent circuit is shown in Fig. 4.5(a). Equivalent circuits when switch is turned on is shown

in Fig. 4.5(b). The inductor current is given by

$$e_a(t) = E_m.\sin \omega t = L_{ba} .\frac{di_{La}}{dt} \qquad (4.16)$$

Equation (4.16) is solved in the interval $\omega t = \alpha$ to $\omega t = \alpha + \omega T_1$ and the expression for the inductor current is given by

$$i_{La}(t) = \frac{E_m}{\omega L_{ba}} \left\{ \cos \alpha - \cos (\alpha + \omega t) \right\} \qquad (4.17)$$

where α is the angle at which boost switch is turned on.

Substituting $i_{La} = I_{2K}$ at $\omega t = \alpha + \omega T_i$

or,
$$I_{2k} = \frac{E_m}{\omega L_{ba}} \left\{ \cos \alpha - \cos (\alpha + \omega T_1) \right\} \qquad (4.18)$$

The differential equation during the interval when the switch is turned off is given by

$$E_m.\sin (\omega t) = L_{ba} \frac{di_{ea}(\omega t)}{dt} + V_{dc} \qquad (4.19)$$
$$\alpha + \omega T_1 < \omega t < \alpha + \omega t_1 + \omega t_2 + \omega T_2$$

or,

$$i_{ea}(\omega t) = I_{2k} + \frac{E_m}{\omega L_{ba}} [-\cos (\omega t)] - \frac{V_{dc}}{\omega L_b} \omega t \qquad (4.20)$$

At $\omega t = \omega T_2$, the inductor (L_{ba}) current becomes zero. Hence,

$$0 = I_{2k} + \frac{E_m}{\omega L_{ba}} [\cos (\alpha+\omega T_1) - \cos (\alpha+\omega T_1+\omega T_2)] - \frac{V_{dc}}{\omega L_{ba}} \omega T_2 \qquad (4.21)$$

Subsituting the value of I_{2k} from equation (4.18) in equation (4.21)

$$0 = \frac{E_m}{\omega L_b}\left[\cos\alpha - \cos(\alpha + \omega T_1 + \omega T_2)\right] - \frac{V_{dc}}{\omega L_b}\omega T_2 \qquad (4.22)$$

$$\text{or,} \quad \omega T_2 = \frac{E_m[\cos\alpha - \cos(\alpha + \omega T_1 + \omega T_2]}{V_{dc}} \qquad (4.23)$$

From equation (4.23) the value of T_2 at which the inductor L_{ba} current goes to zero can be calculated. The maximum value of T_2 is equal to $(1 - D)T_s$. This can be computed by switching on the boost switch at the peak input voltage (E_m). Under this condition the current through the inductor (L_{ba}) increases at its maximum rate and reaches to maximum value at the end of ωT_1. Also, the time required for the current (i_{La}) to fall to zero is maximum. Therefore, the switching frequency of the switch is a function of ac input voltage (e_a) and output dc voltage (V_{dc}). Substituting $\alpha = 90^\circ$ in equation (4.7). The expression for inductor current is given by

$$i_{ea}(\omega t) = \frac{E_m}{\omega L_{ba}}\sin(\omega t) \qquad (4.24)$$

At time T_1 the inductor current (i_{ea}) reaches its maximum value and the boost switch is turned off. Substituting $\alpha = 90^\circ$ in equation (4.22) yields,

$$\frac{E_m}{\omega . L_{ba}}\sin(\omega T_1 + \omega T_2) - \frac{V_{dc}}{\omega . L_{ba}} . \omega T_2 = 0 \qquad (4.25)$$

Since switching frequency is very high compared to line frequency $(\omega T_1 + \omega T_2)$ will be very small, hence $\sin(\omega T_1 + \omega T_2)$

$\simeq (\omega T_1 + \omega T_2)$.

or $$E_m.(\omega T_1 + \omega T_2) = V_{dc}.\omega T_2$$

or $$E_m(T_1 + T_2) = V_{dc}\, T_2 \qquad (4.26)$$

Since its operating for $\alpha = 90^\circ$, T_3 is '0', therefore, maximum permissible value of D for given value of peak input voltage (E_m) and output voltage V_{dc} can be determined from equation (4.26). The maximum value of D is given by

$$D_{max} = \frac{V_{dc} - E_m}{V_{dc}} \qquad (4.27)$$

For this D_{max}, the peak current in boost inductor can be obtained from equation (4.18) and is given by

$$I_{2k} = \frac{E_m}{\omega.L_{ba}} . \sin \omega T_1$$

where $\sin \omega T_1 \simeq \omega T_1$

or, $$L_{ba} = \frac{E_m.t_1}{I_{2k}}$$

where $t_1 = DT_s$.

or, $$L_{ba} = \frac{E_m.DT_s}{I_{2k}} \qquad (4.28)$$

or, $$L_{ba} = \frac{E_m.D}{I_{2k}.F_s} \qquad (4.29)$$

where F_s is switching frequency.

The conclusions drawn from the above analysis are

(1) The size of boost inductor is inversely proportional to switching frequency.

(2) For discontinuous mode of operation, the relationship between the output voltage, duty cycle and peak input voltage is given by equation (4.27).

For a given duty ratio, the minimum value of output voltage which will result in discontinuous mode of operation can be determined by this equation.

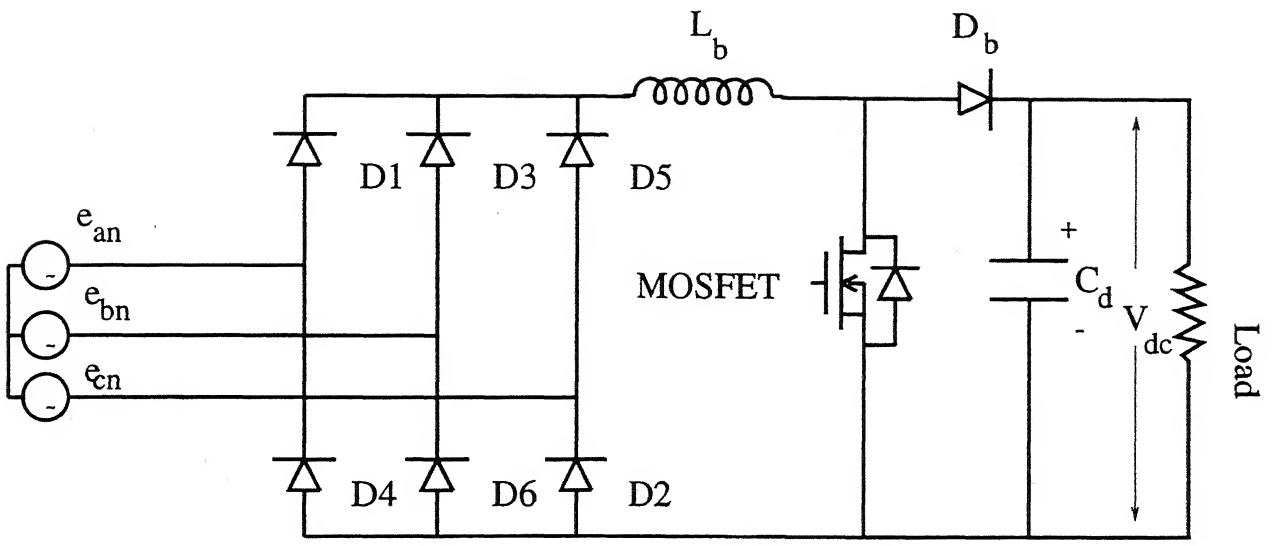

Fig 4.1 three-phase boost rectifier with boost inductor on dc side

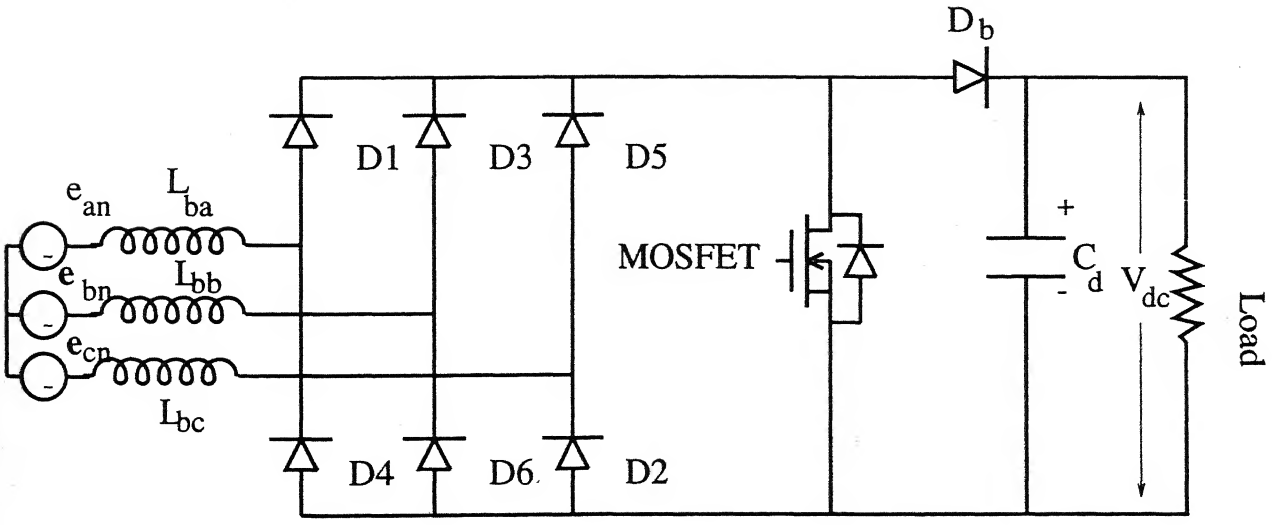

Fig 4.2 Three-phase boost rectifier with boost inductor on ac side

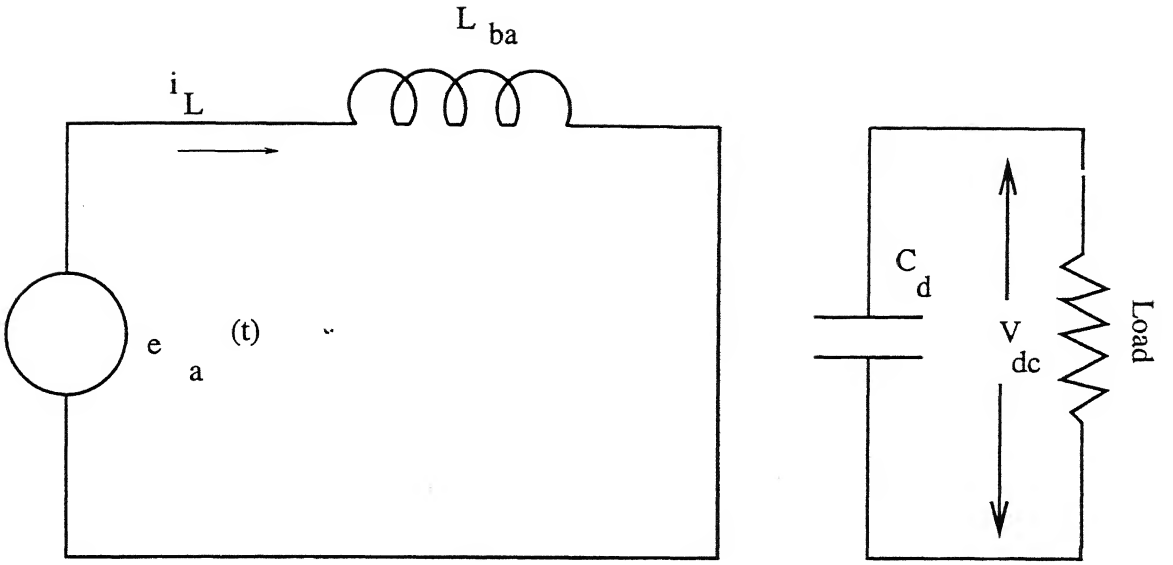

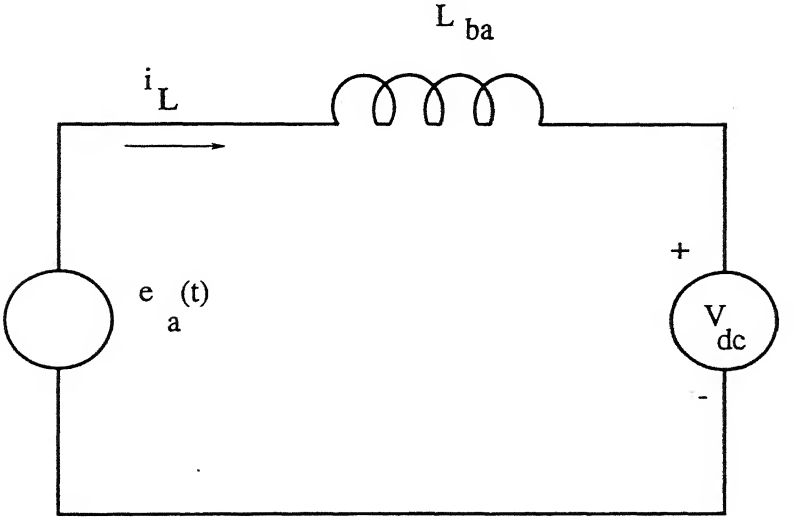

(b)

Fig 4.3 equivalent circuit of boost rectifier of Fig 4.1

(a) Equivalent circuit with SW on (b) Equivalent circuit with SW ofb

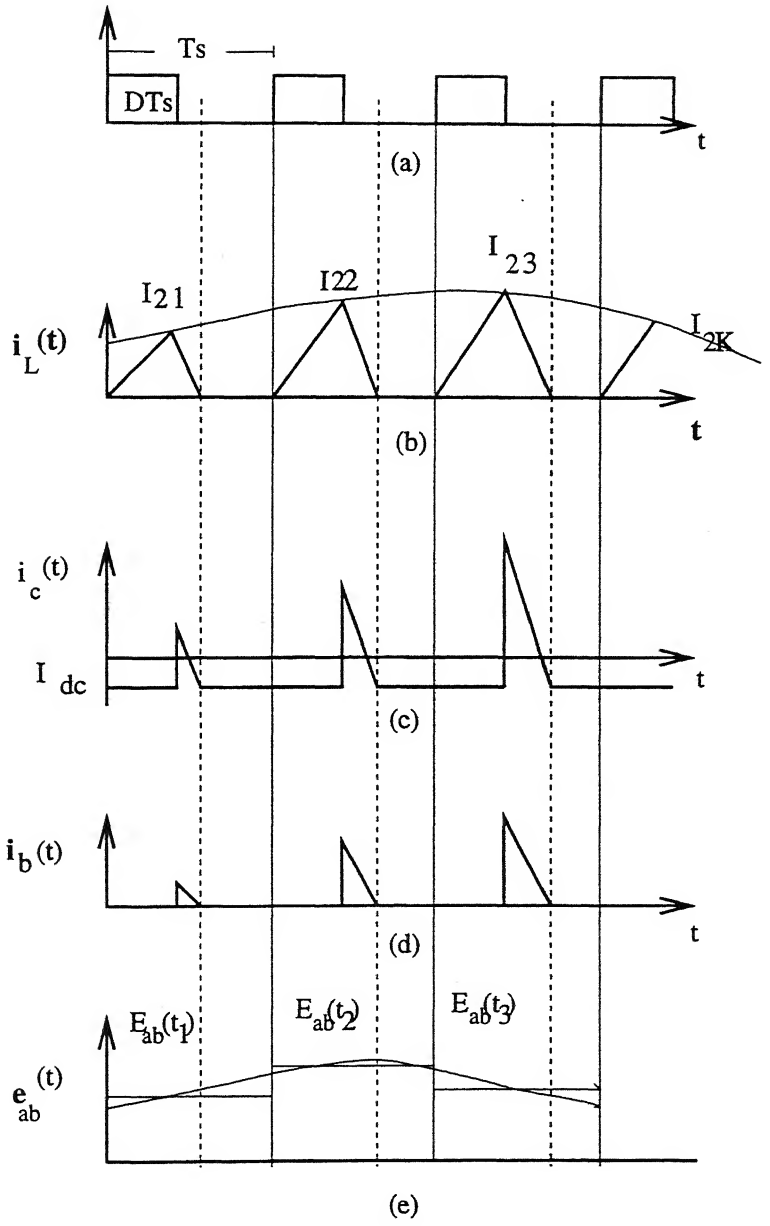

Fig 4.4 Waveforms of gating signals and some corresponding voltage and current waveforms

(a) Gating signals (b) Boost inductor current

(c) Capacitor C_d current (d) Boost diode current

(e) Waveform of $e_{ab}(t)$

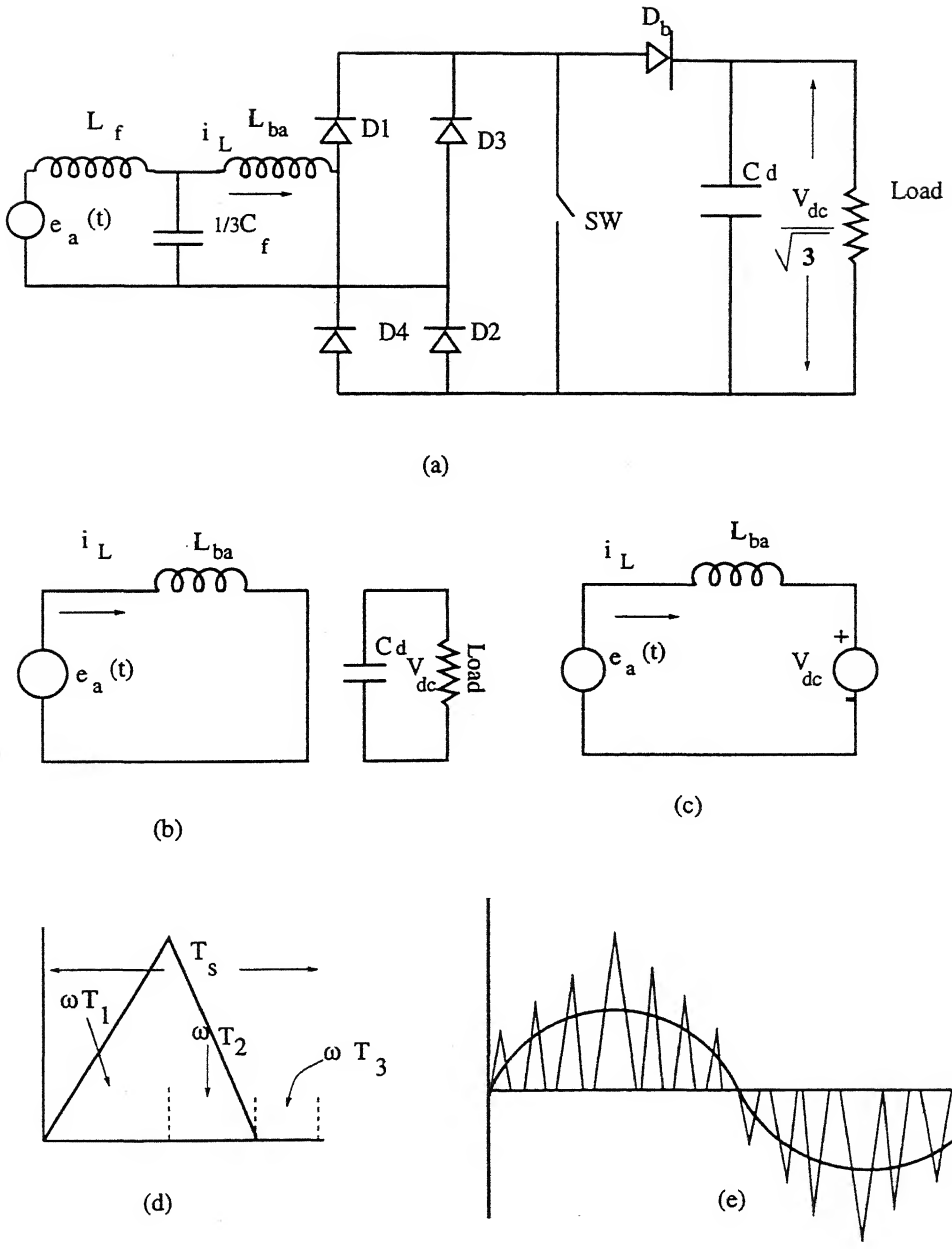

Fig 4.5 equivalent circuit of boost rectifier of Fig 4.2 and boost inductor current

(a) Single - phase equivalent of boost rectifier of Fig 4.2

(b) Equivalent circuit with SW on (c) Equivalent circuit with SW off

(d) Magnified boost inductor current (e) Boost inductor current

CHAPTER - FIVE

DESIGN AND SIMULATION

5.1 Design of Converter

The value of boost inductor is determined as follows. When the boost switch is turned on, L_b should be large enough to limit the current to I_p (maximum Device current) given by equation,

$$I_{2k} = E_a(t_k)\left[\frac{(k+D)T_s}{L_b}\right] < I_p \qquad (5.1)$$

$$k = 1, 2, \ldots., n.$$

Taking the maximumum of $E_a(t_k)$, the boost indicatance is

$$L_b > \frac{E_m}{I_p} D_m T_s \qquad (5.2)$$

where D_m is the maximum possible duty ratio.

The current in inductor is always discontinuous, therefore,

$$1 - D_m - D_{1k} > 0 \qquad k = 1, 2, \ldots., n \qquad (5.3)$$

When switch is turned off

$$L_b \frac{di_L}{dt} = E_a(t_k) - V_{dc} \qquad (5.4)$$

Assumming that the current decreases linearly,

$$L_b \Delta i_L = \left[E_a(t_k) - V_{dc}\right] D_{1k} T_s \qquad (5.5)$$

From (5.3) and (5.5)

$$1-D_m - \frac{L_b . \Delta i_L}{[e_a(t_k)-V_{dc}]D_{1k}T_s} > 0$$

or
$$L_b < \frac{(1-D_m)[E_a(t_k) - V_{dc}]T_s}{\Delta i_L} \qquad (5.6)$$

Current in the inductor is maximum when source voltage is maximum. If the maximum value of the current is I_m, then,

$$L_b < \frac{(1 - D_m)\ (V_{dc} - E_m)\ T_s}{I_m}$$

The highest value of V_{dc} is selected such that $I_m < I_p$. From equation (5.3) and (5.7).

$$V_{dc} > \frac{E_m}{(1 - D_M)} \left[1 - D_m + \frac{I_m}{I_p} D_m \right]$$

For I_p = 30 A and I_m = 25 A it is found that,

0.117 mH < L_b < 0.143 mH

The corresponding value of V_{dc} should be greater than 140 V. The value of output filter capacitor is obtained by solving (3.18). However, an approximate value can be obtained from (3.22). For 5V ripple, the approximate value of C_d is found to be 2000 μF. However for simulation 1550 μF capacitor is used.

The input filter is designed as suggested in [11] and values of L_f and C_f are found to be 10 mH and 30 μF respectively.

5.2 PSPICE SIMULATION

The converter topologies shown in Fig. 3.1, 3.2, 4.1 and 4.2 are simulated using PSPICE package. Resistance of 0.1 ohm is included in series with each active and passive component to make simulation studies more realistic. The Fast recovery diode is modeled by suitably changing transit time (TT) of standard diode model. IRF 150 MOSFET parameters are used for boost switch model. All passive devices are assumed to be ideal and load is purely resistive.

The performance of different boost rectifiers is studied during steady state and transient period as well.

5.2.1 Simulating Results of Single-Phase Boost Rectifier

The currents in the boost inductor, switch and boost diode during starting for two supply cycles are shown in Fig. 5.1. The steady state has been reached in less than half a cycle. The duty ratio is such that the current is discontinuous. During starting, since the output voltage has not developed, the inductor current becomes continuous for a short period. The output dc voltage, source voltage and current plots are shown in Fig. 5.2. The output voltage has second harmonic component. This is because, when the instantaneous input voltage is small (near Zero crossing) energy transfer to the capacitor is negligible. Capacitor C_d supplies the load current even when the switch is turned on, particularly during the end of a half cycle. Thus, this phenomenon occurs twice per line cycle near zero crossing.

The magnitude of harmonic can be reduced either by increasing C_d or by closed loop control.

The current drawn from source is nearly sinusoidal and in phase with input voltage. The magnitude of initial transient current is high. Therefore devices with high rating should be used in order to avoid the device failure. The harmonic distortion of the input current is found to be around 3% and power factor and displacement factor are found to be very close to unity (0.9995).

The Fig. 5.3 and 5.4 show the waveforms for circuit configuration shown in Fig. 3.2. The rectified voltage is applied to boost inductor. This results in average dc current in inductor. Due to this air core shuld be used to avoide core saturation.

The following observations are made -

(i) The current drawn from supply is nearly sinusoidal and in phase with source voltage.

(ii) The output voltage has second harmonic component. In order to reduce the harmonic content either high value of filter capacitor should be used or suitable close loop should be designed which increases the value of D near the zero crossing of supply voltage.

(iii) Devices with high current rating should be selected to avoid the device failure.

(iv) Since the average current in the inductor is zero for the circuit shown in Fig. 3.1, smaller core can be used.

This results in further reduction in the size of equipment.

5.2.2. Simulated Results of Three-Phase Boost Rectifier

Fig. 5.5 shows the variation of current in boost inductor, boost diode, capacitor and diode in three-phase bridge. The variation of these currents at reduced time scale is shown in Fig. 5.6. Though the magnitude of initial current is quite high during starting, it reaches the steady stave value within one cycle. The magnitude of current in boost inductor is the sum of the currents in three phases. Therefore, boost inductor should have higher rating. Each diode in the bridge conduct for $2\pi/3$ radian per cycle.

The variation in output voltage, input voltage and current are shown in Fig. 5.7. Since diode in bridge conducts for $2\pi/3$ radian in each line cycle, the current drawn from source is non-sinusoidal. However fundamental component is in phase with input voltage. Total harmonic distortion is around 10% and power factor is around 0.97. The magnitude of harmonic current is given in Table 2.

The simulated results of the circuit shown in Fig. 4.2 are shown in Fig. 5.9 and 5.10. The ripple in output voltage is negligibly small and current drawn from the source is sinusoidal. In steady state the source current is in phase with input voltage. The current waveform through three boost inductor is shown in Fig. 5.10. The diode in rectifier bridge conduct for π radian per cycle. The total harmonic distortion

for this circuit configuration is found to be around 4% and input power factor is 0.98. The harmonic content in supply current is shown in Table 3.

The effect of D on supply current is studied and results for 0.3, 0.6 and 0.8 are shown in Fig. 5.11. It is found that for values of D less than D_{max} current in boost inductor is discontinuous.

However for D greater than D_{max}, the boost inductor current becomes continuous and output voltage decreases. The reason for decrease in output voltage is, that only partial energy transfer from inductor to output capacitor and load takes place. The harmonic content in input current increases with D. This results in decrease in power factor. The inductor current for D = 0.6 and 0.8 are shown in Fig. 5.12(a) and (b) respectively. Based on simulation studies the observations made are,

(i) Rectifier draws nearly sinusoidal current from mains at unity power factor.

(ii) The output dc voltage has very low ripple.

(iii) The steady state is reached in less than a supply cycle.

5.3 TABLE OF HARMONIC ANALYSIS OF INPUT CURRENT

Table 1

The magnitude of Harmonic Component of Single-Phase Boost rectifier with boost inductor on ac side.

Fundamental component of input current 5.426 A, Displacement angle = 13.286°

Harmonic No.	Fourier Component in Amp.
1	5.426
2	0.1256
3	0.0151
4	0.0822
5	0.0497
6	0.0184
7	0.0692
8	0.0250
9	0.0606

Total harmonic distortion (THD) = 3.38%

$$\text{Power factor} = \frac{I_A}{\sqrt{\sum I_h^2}} \times \text{displacement factor}$$

or, PF = 0.973

Table 2

Magnitude of Harmonic Component of input current of three-phase boost rectifier with boost inductor on dc side.

Fundamental Component of input current = 6.349 A, Displacement angle = 7.5°

Harmonic No.	Fourier Component in Amp.
1	6.349
2	0.00365
3	0.0042
4	0.00123
5	0.9377
6	0.0022
7	0.0306
8	0.0012
9	0.0012

Total harmonic distortion (THD) = 15%

PF = 0.98

Table 3

Magnitued of Harmonic component of input current of three-phase boost rectifier with 3 boost inductors on ac side

Fundamental component = 11.0 Amp.

Harmonic No.	Fourier Component in Amp.
1	11.0000
2	0.3972
3	0.1101
4	0.0249
5	0.0824
6	0.0295
7	0.0564
8	0.0233
9	0.0139

Total harmonic distortion (THD) = 3.87%

PF = 0.98

Table 4

Experimental Result.

Variation of output voltage with duty ratio. Line to line input voltage 40 V (rms).

D	Output
0.3	80 V
0.4	88 V
0.5	100 V
0.6	95 V
0.7	90 V

Boost inductor current becomes continuous for values of D > 0.5.

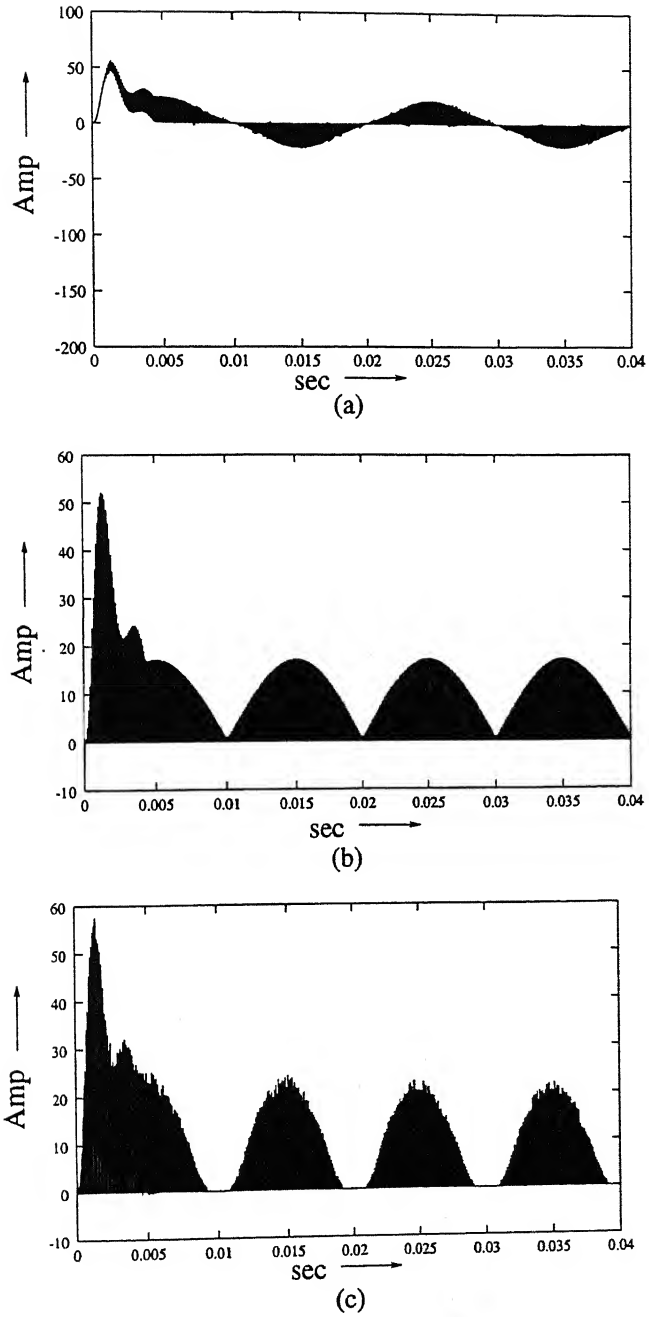

Fig 5.1 Waveforms of boost converter of Fig 3.1

(a) Boost inductor current (b) Boost switch current

(c) Boost diode current

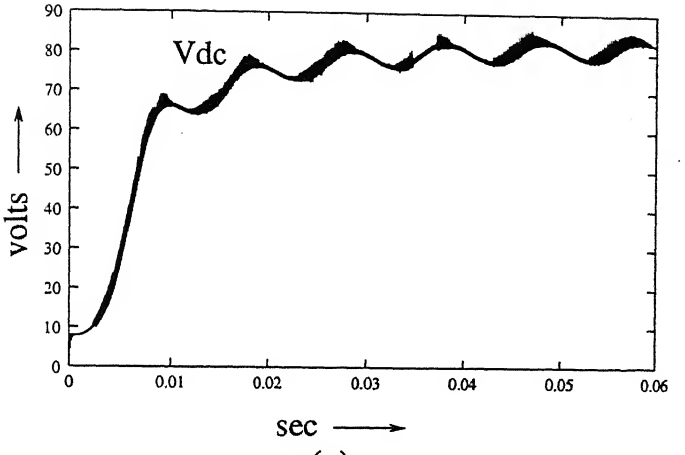

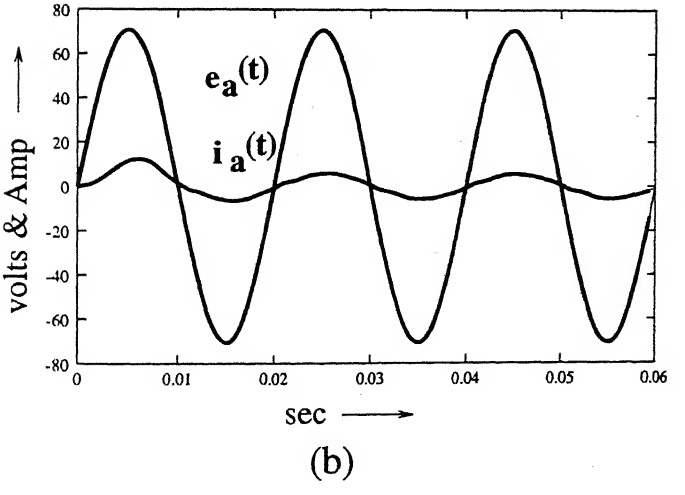

Fig 5.2 Waveforms of boost rectifier of Fig 3.1

(a) Output voltage (b) Source voltage - source current

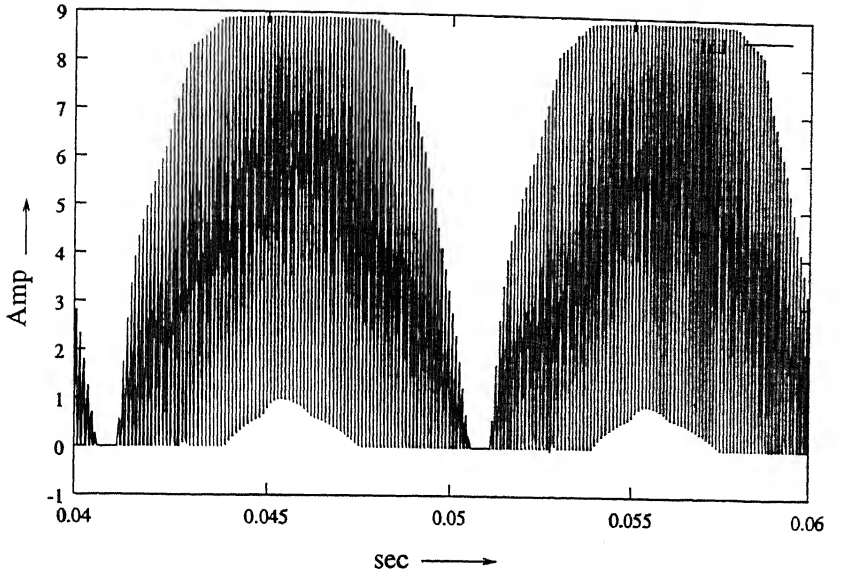

(a)

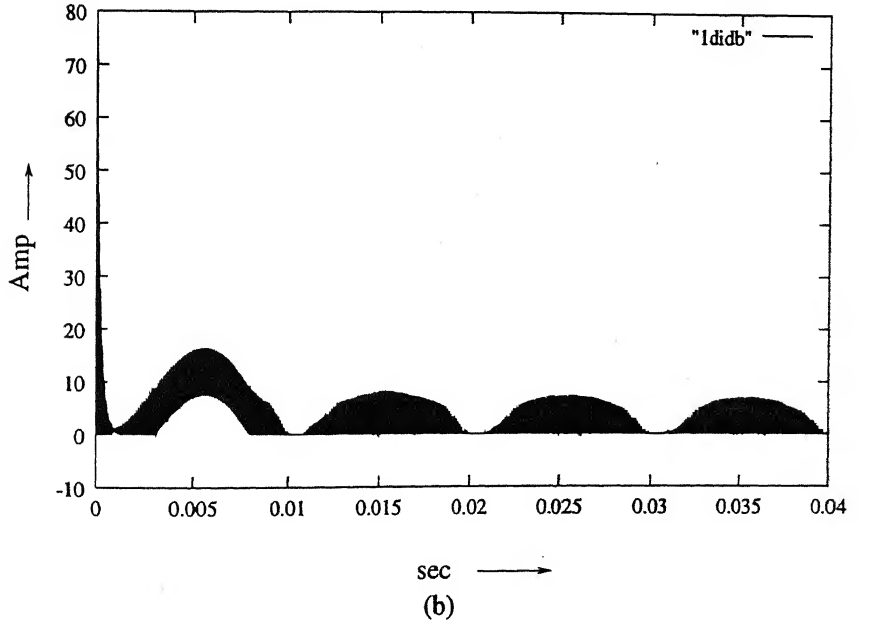

(b)

Fig 5.3 Waveforms of boost rectifier of Fig 3.2

(a) Boost inductor current (b) Boost diode current

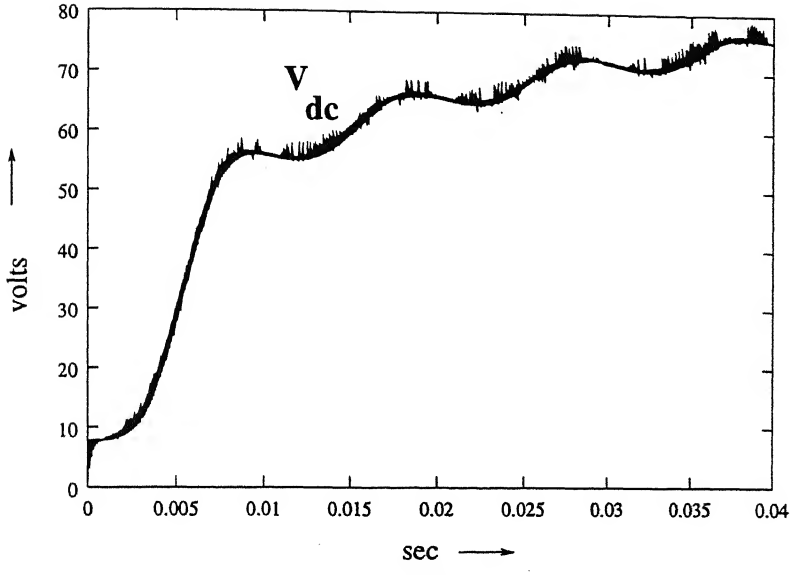

(a)

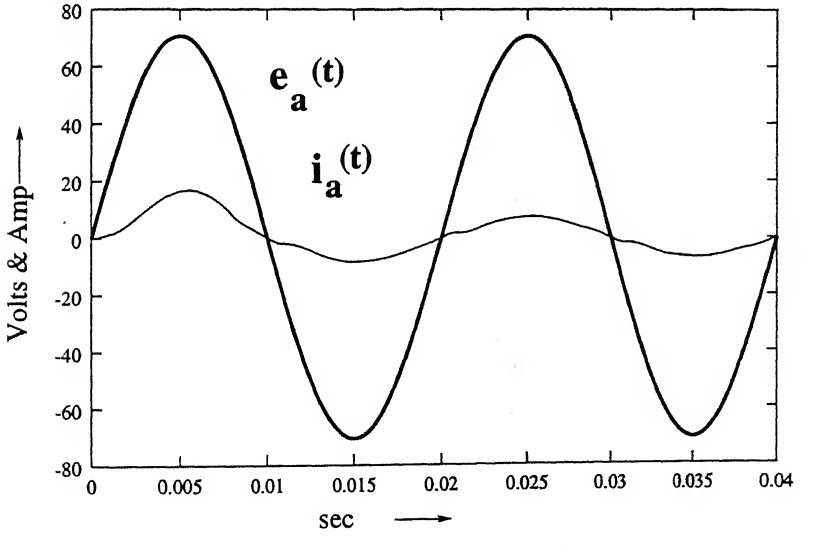

(b)

Fig 5.4 Waveforms of boost converter of Fig 3.2

(a) output voltage (b) input voltage - input current

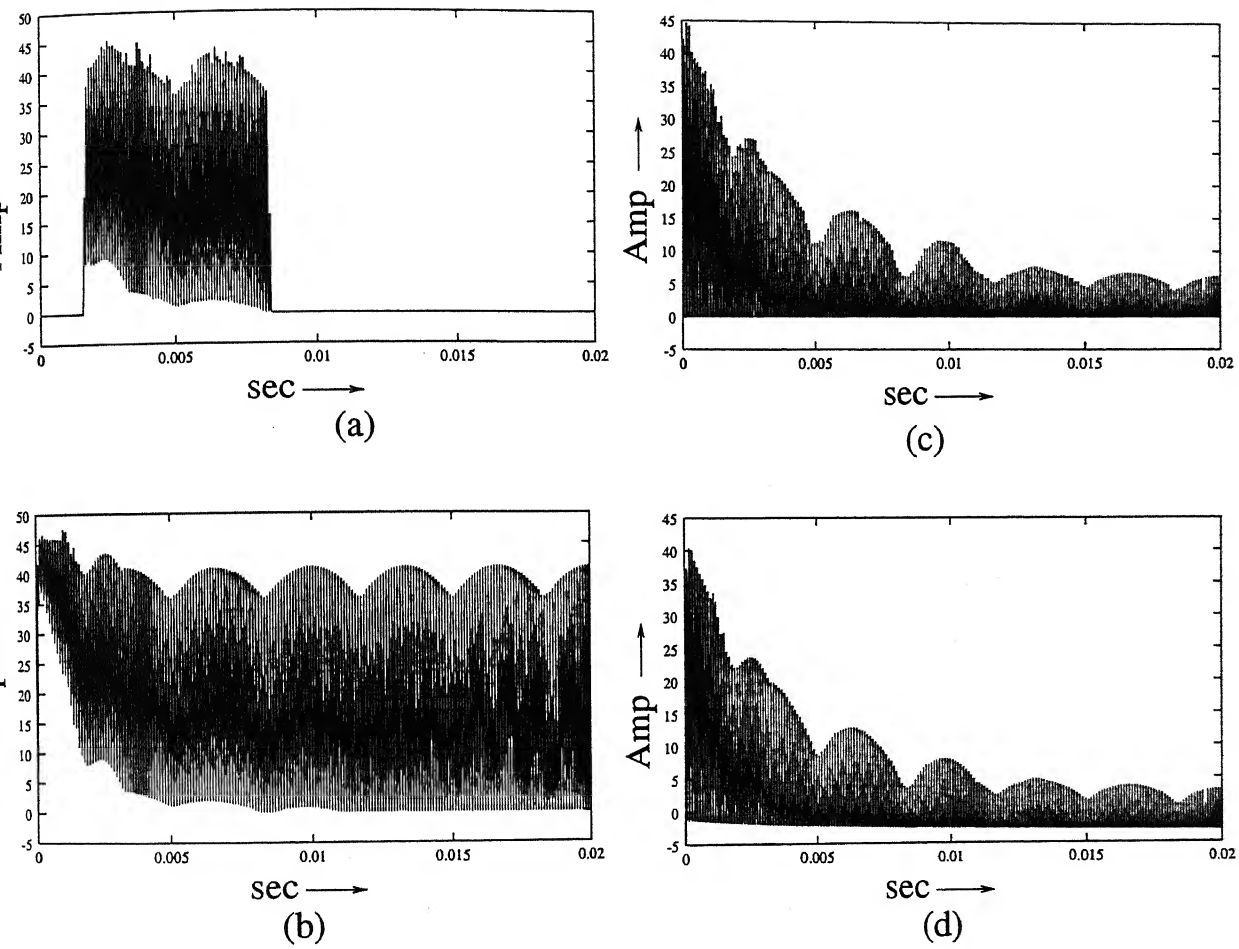

Fig 5.5 Waveform of three-phase boost converter of Fig 4.1

(a) Bridge diode current (b) Boost inductor current

(c) Capacitor current (d) Boost diode current

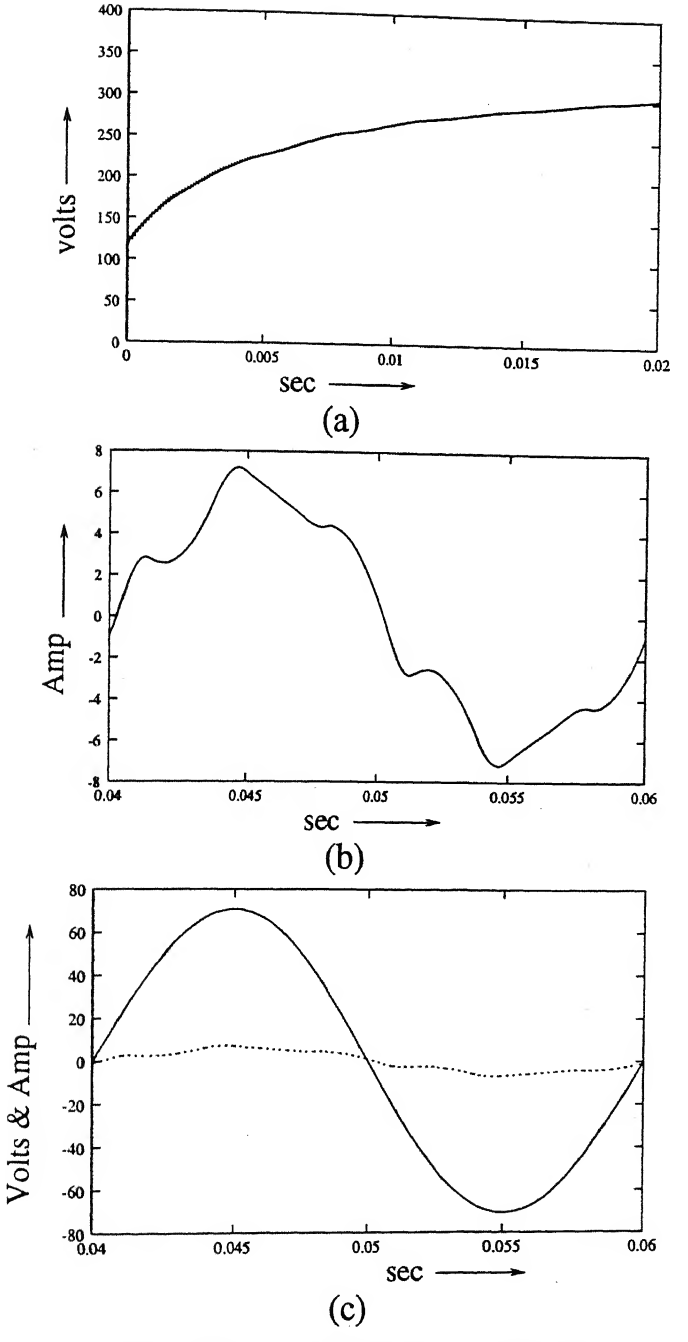

Fig 5.7 Waveform of converter of Fig 4.1

(a) Out put voltage (b) Magnified source current

(c) Source voltage - source current

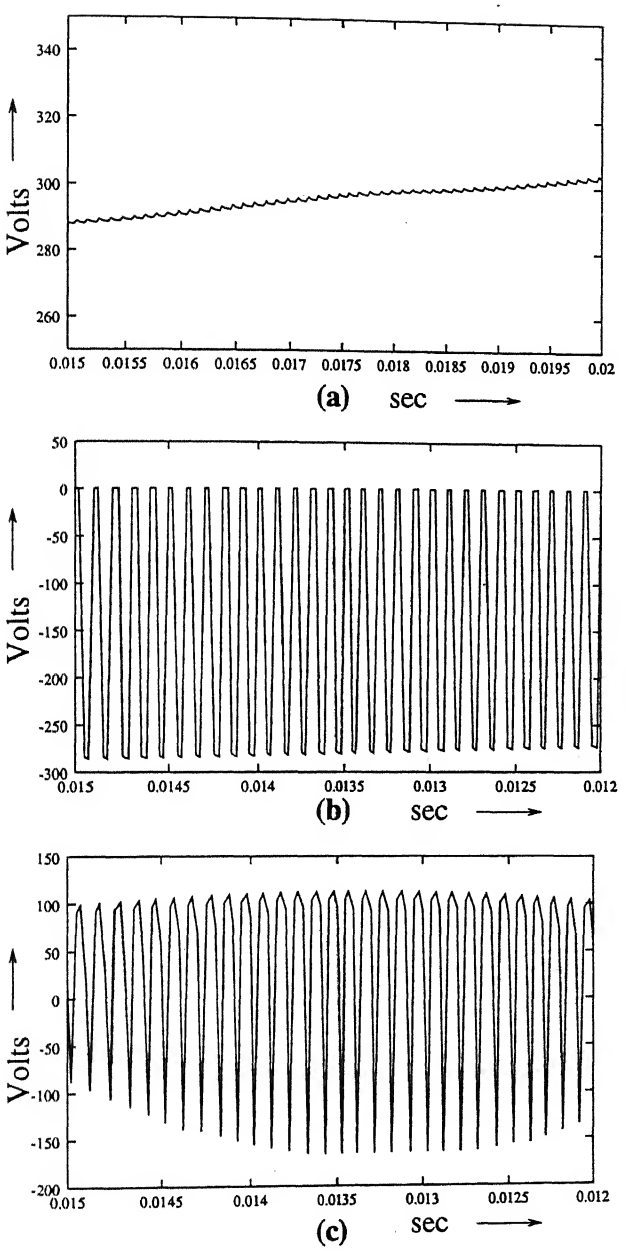

Fig 5.8 Voltage waveforms of boost converter of Fig 4.1

(a) Out put voltage (b) Voltage across boost diode

(c) Voltage across boost inductor

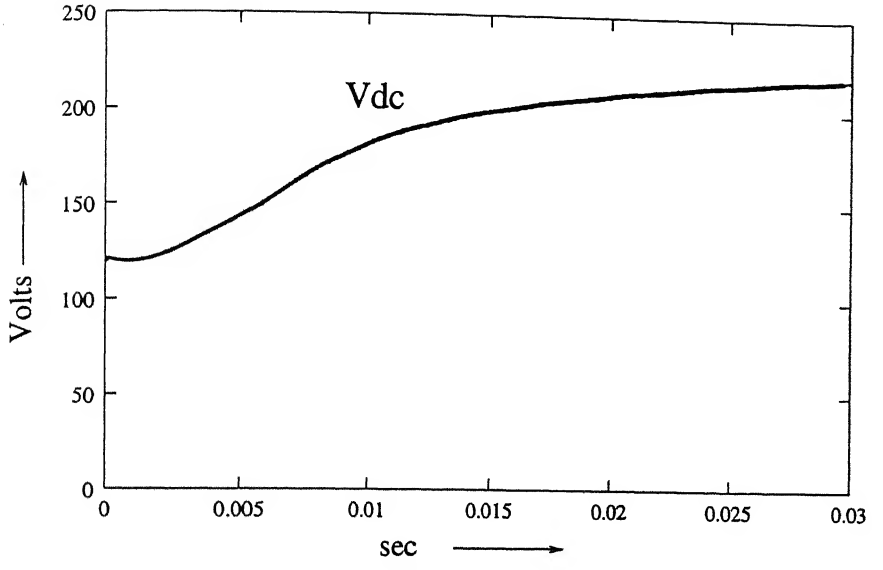

(a)

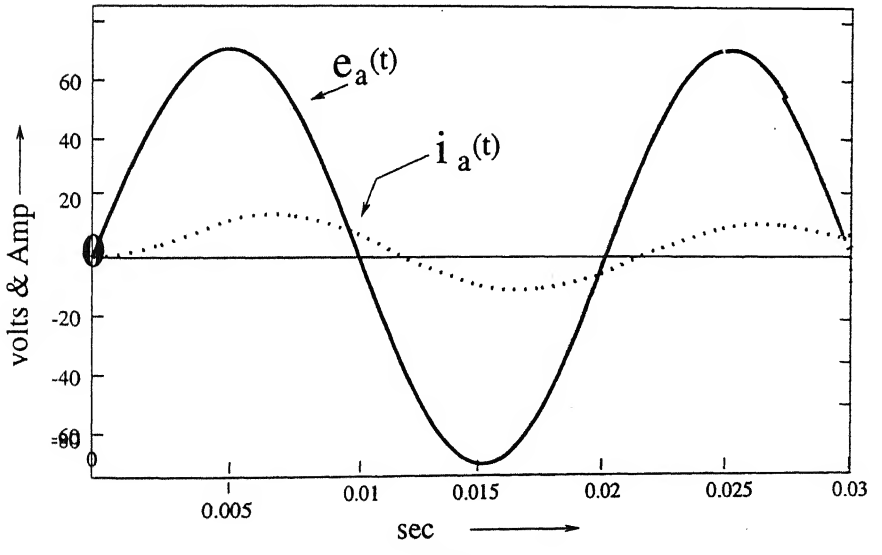

(b)

Fig 5.9 Waveforms of boost converter with inductors on ac side of Fig 4.2

(a) Output voltage (b) Source voltage and current of phase 'a'

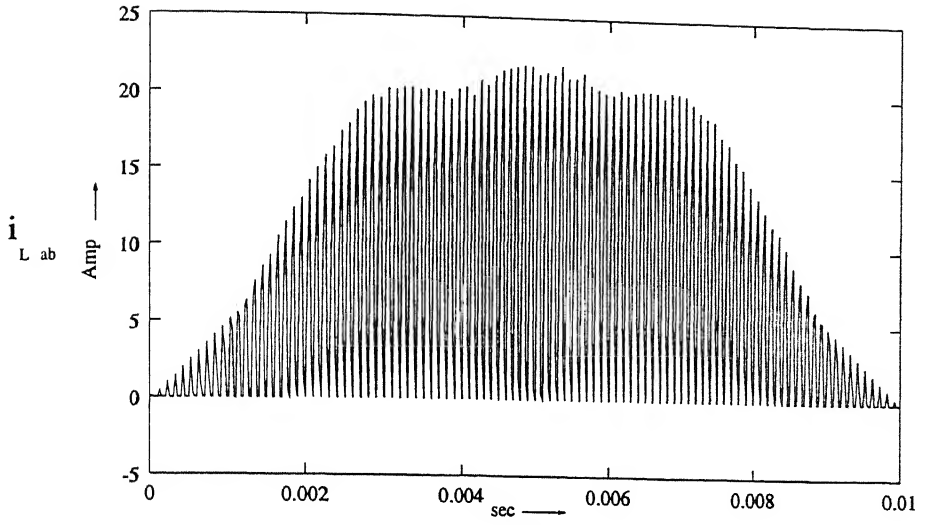

(a)

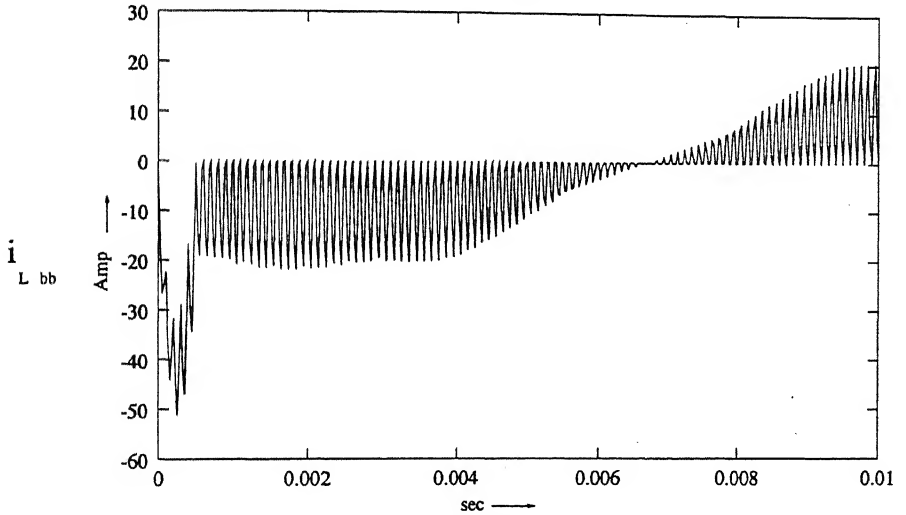

(b)

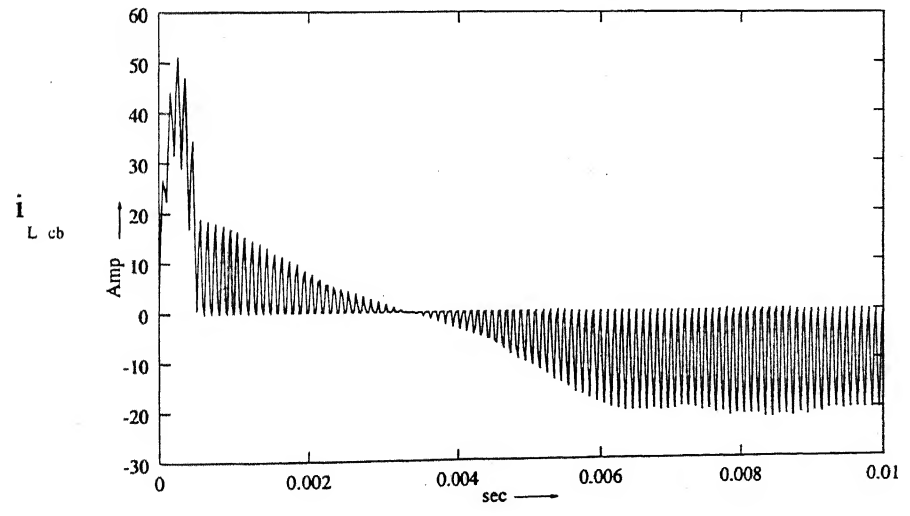

(c)

Fig 5.10 Boost inductor current waveforms of boost converter of Fig 4.2

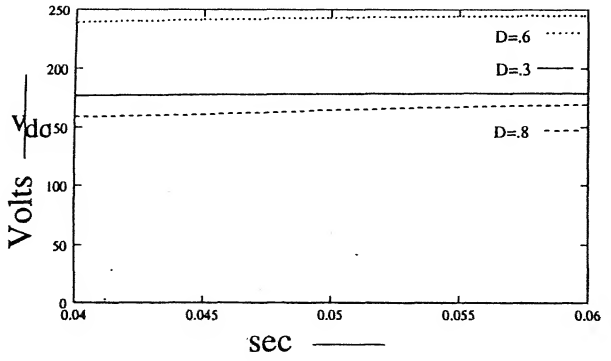

(a)

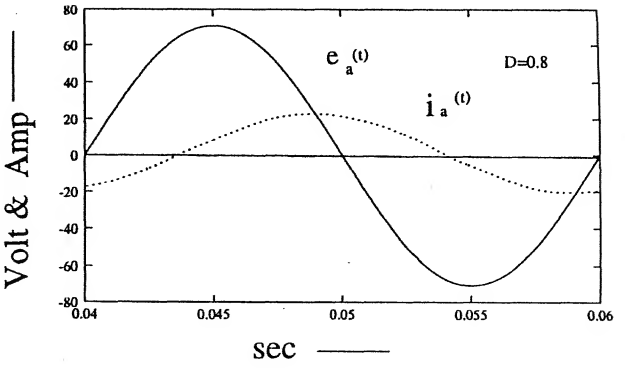

(c)

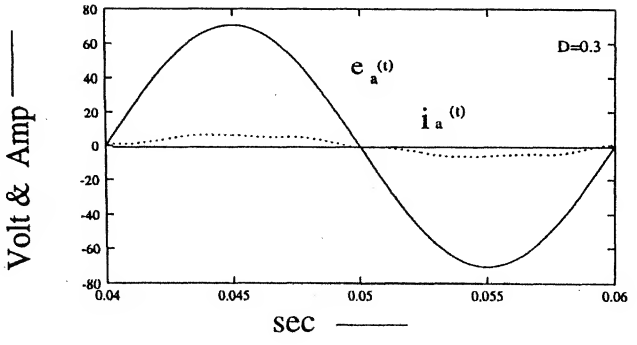

(b)

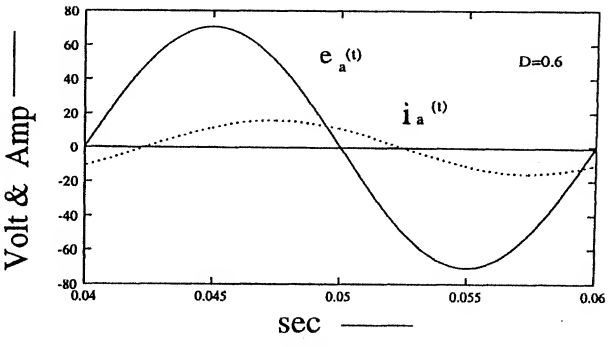

(d)

Fig 5.11 Source voltage and current plot of boost converter of Fig 4.2

(a) Output voltage for D=0.3 ,0.6.,0.8 (b), (c), (d) Phase voltage - current Plot

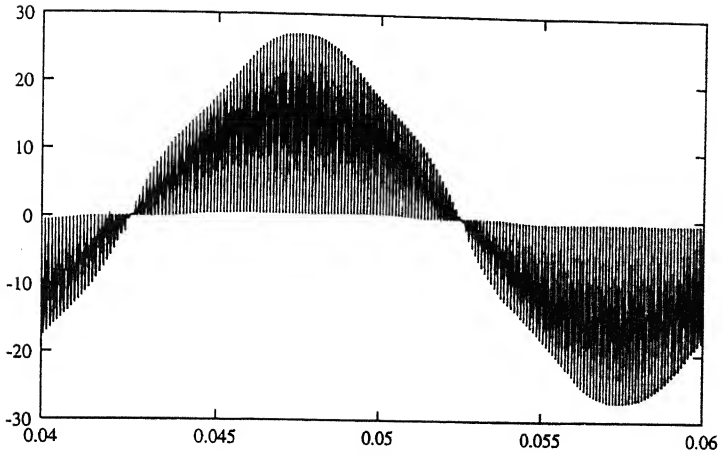

(a)

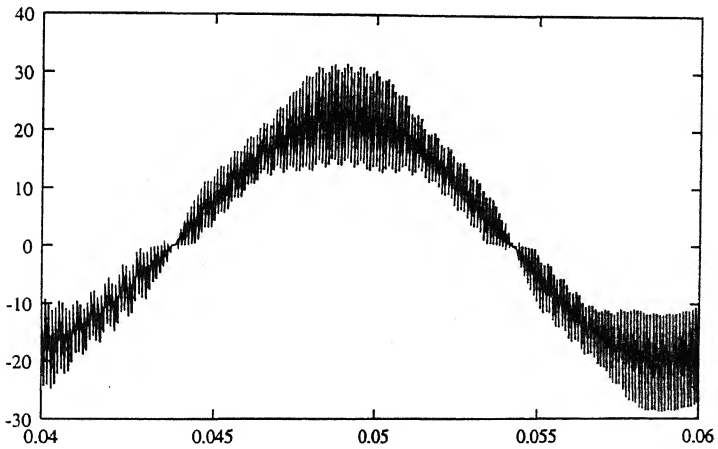

(b)

Fig 5.12 Boost inductor current variaion with duty ratio

(a) D=0.6 (b) D=0.8

CHAPTER SIX

IMPLEMENTATION AND CLOSED LOOP CONTROL

6.1 INTRODUCTION

Based on design parameters and simulation results a proto type of three phase boost rectifier, with boost inductor on AC side is fabricated. The block diagram of overall experimental set up is shown in Fig. 6.1.

The bridge rectifier comprises of six fast recovery diode. Air core inductor of 0.122 mH is used as boost inductor. The active wave shaping stage is built by MOSFET (IRF50PE) and fast recovery diode (FR 306). The important point to be observed here is that switching characteristics of the MOSFET and the boost diode should be approximately the same. Otherwise it may result in voltage spikes across boost diode and switch which may destroy the devices. Suitable snubber circuits are used to reduce the heating of device.

6.2 CONTROL AND GATE DRIVE

The gate pulses are generated by comparing a constant dc voltage with high frequency triangular pulses. IC 566 function generator is used for generating the triangular wave. The frequency of these pulses can be varied by varying R_3 and C_1. D is varied by changing the dc level. The control circuit which drives the MOSFET is shown in Fig. 6.3. Variation of output voltage with D is shown Table 4.

6.3 FEEDBACK CONTROL

Any fluctuation in input supply current or load will result in variation of output voltage. The converter operates at fixed value of D in steady state condition. Fig. 6.2 shows the block diagram of control circuit used to maintain voltage constant. Here the output voltage is compared with a fixed reference voltage. The error voltage is added to normal value of D_o to provide required $D_o \pm \bar{D}$ where $\pm \bar{D}$ corresponds to change in duty ratio of switch to bring back the output voltage to the original value.

The gain of error amplifier has been selected by trial and error method. It is found that a gain between 2 to 3 gives satisfactory performance.

A sample and hold network has been used, which sences the output voltage at the begining of each switching cycle and maintains the dc level constant.

For guarenteeed discontinuous mode of operation, protection of switch and associated circuit limiter has been used to limit the maximum value of duty ratio below maximum permissible value of D.

6.4 TEST RESULTS

The converter is tested extensively with dc load varying from 100Ohms to 200 Ohms. The wave forms of boost switch current, boost inductor current, boost diode current, input voltage and input currents are recorded for D= 0.5. Fig. 6.5 - 6.8 show the experimental oscillograms.

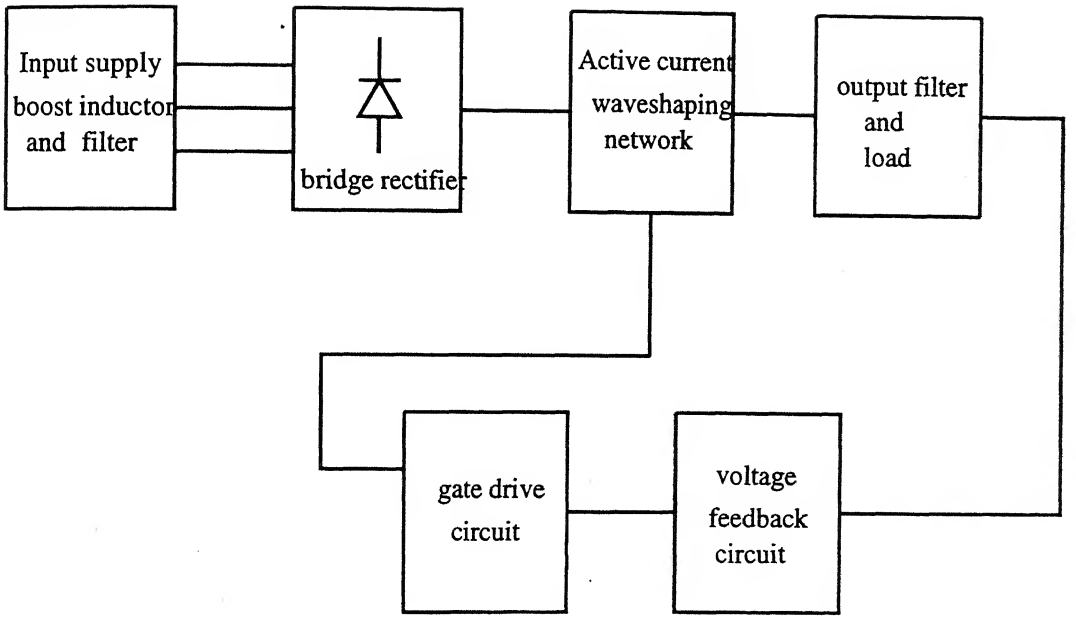

Fig 6.1 Block diagram of experimental setup

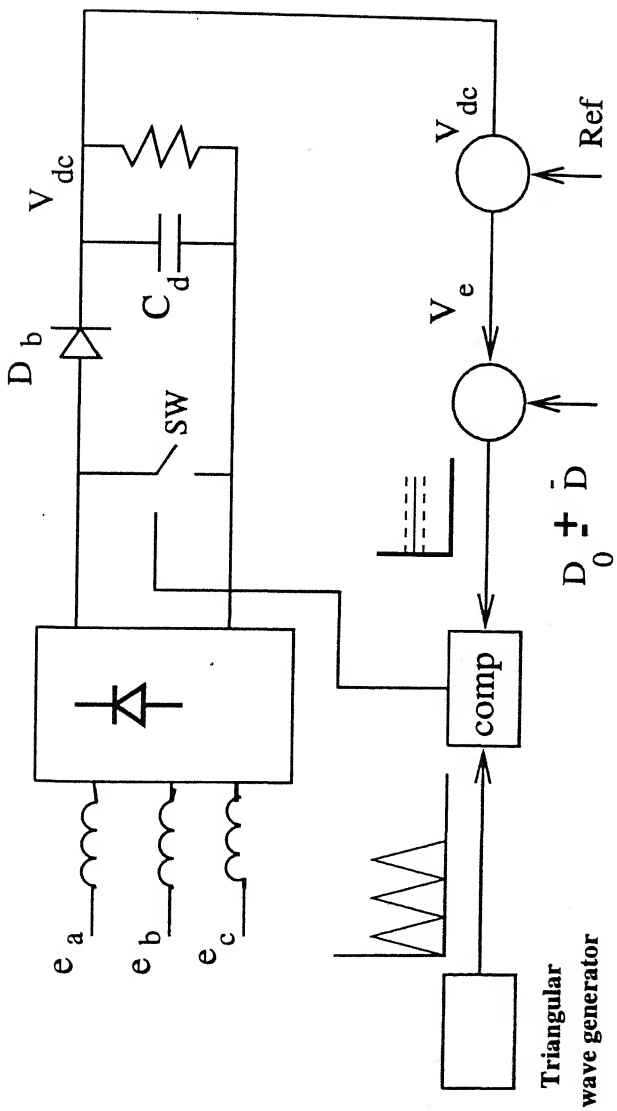

Fig 6.2 Control circuit block diagra

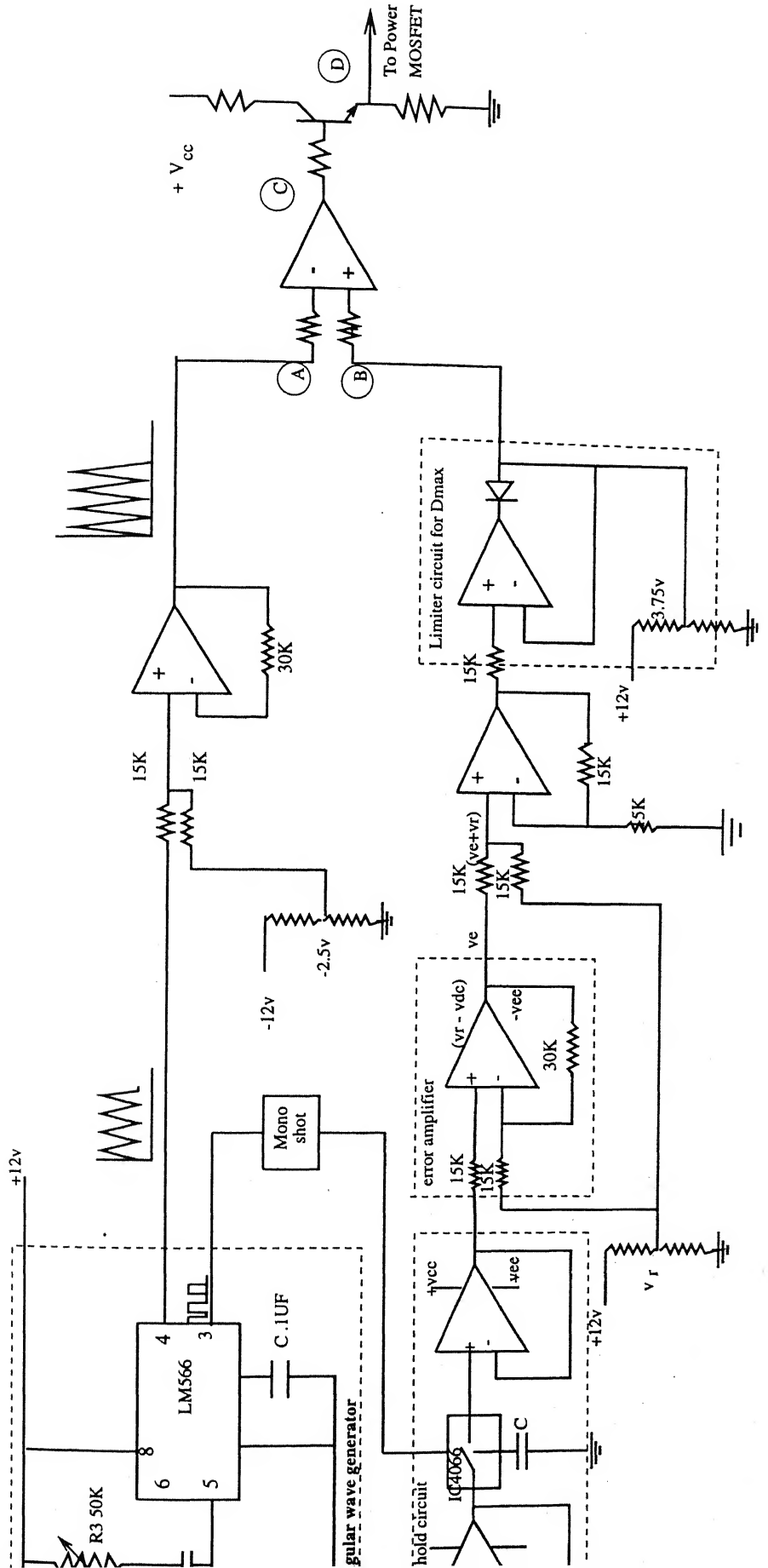

Fig 6.3 control circuit for boost rectifier

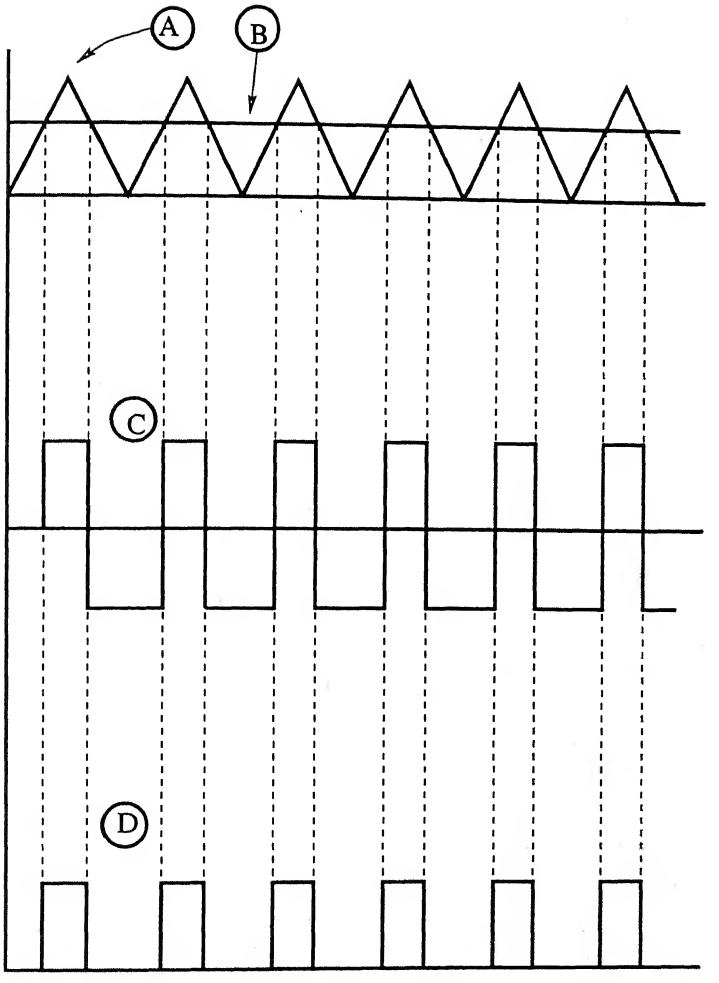

Fig 6.4 Gate pulse signal for power MOSFET

(A) High frequency triangular wave (B) D C referance signal

(C) Output of comperator (D) Gate pulsefor MOSFET

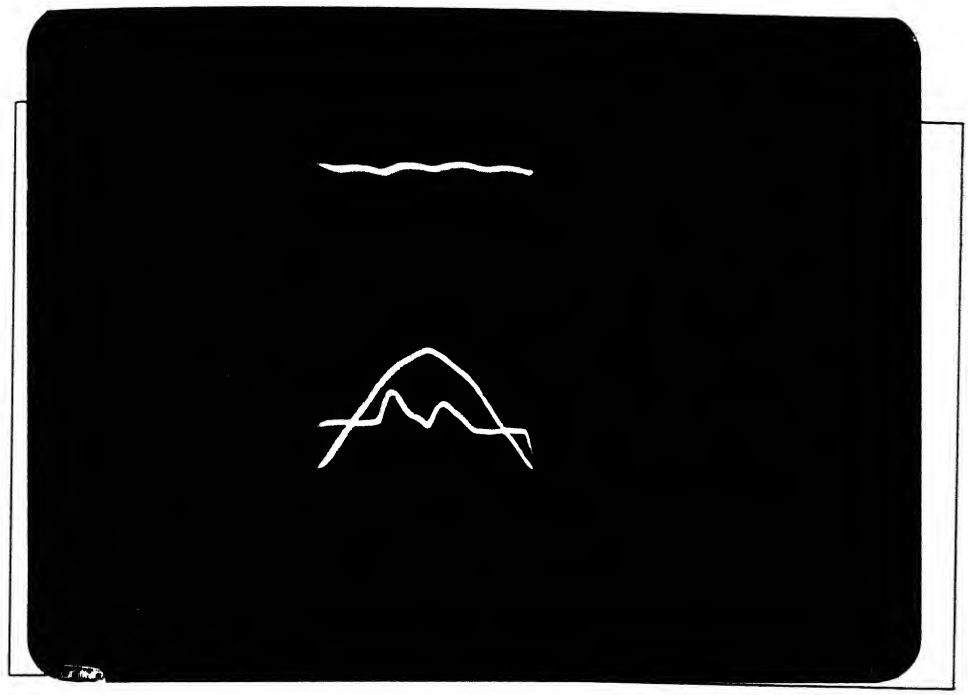

(a)

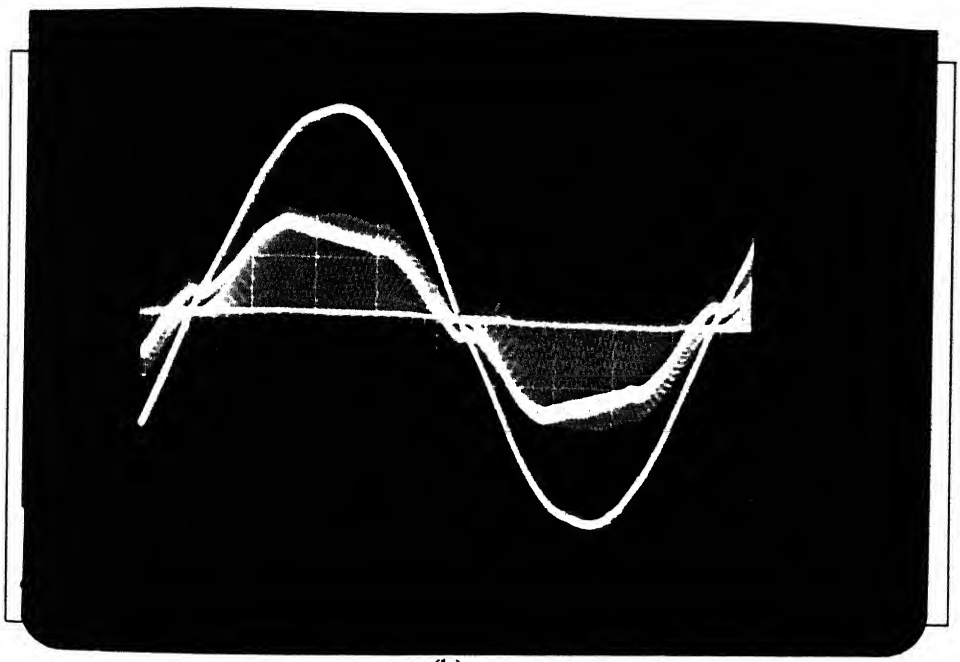

(b)

fig 6.5 Experimental oscillogram duty 0.5

(a) Output voltage source current and source voltage without active waveshaping

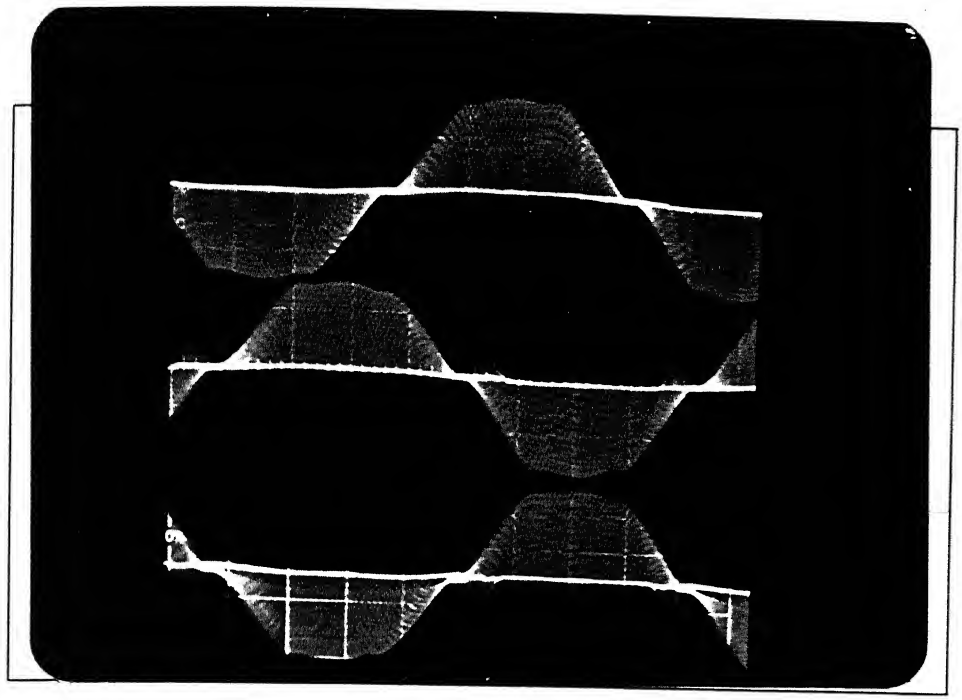

(a)

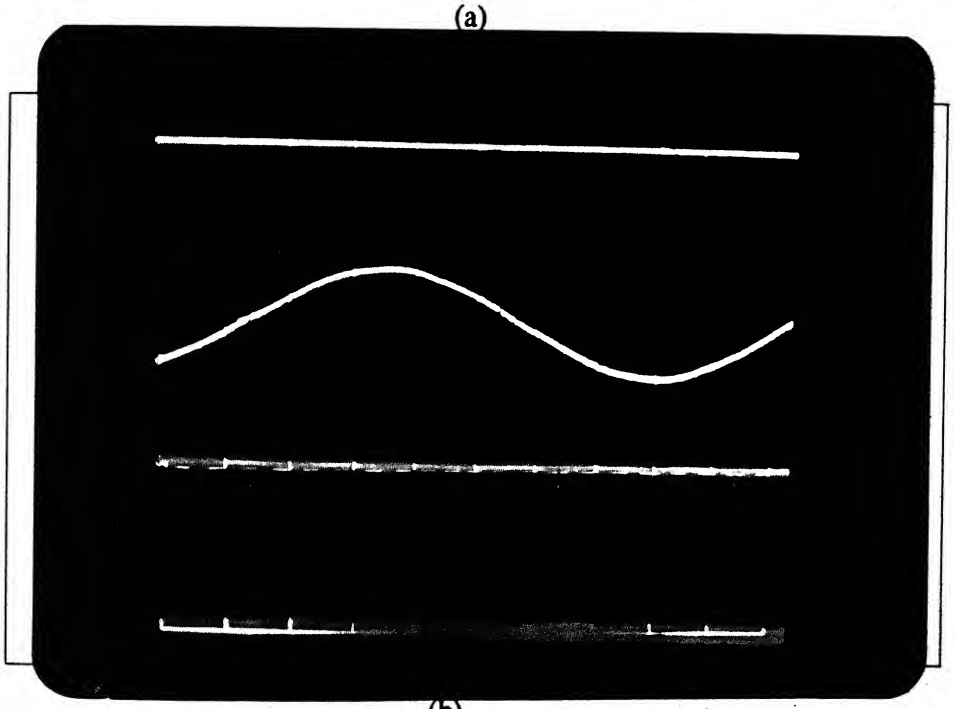

(b)

fig 6.6 Experimental oscillogram duty 0.5

(a) Boost inductor current of three phases

(b) Output voltage source voltage and gate pulses

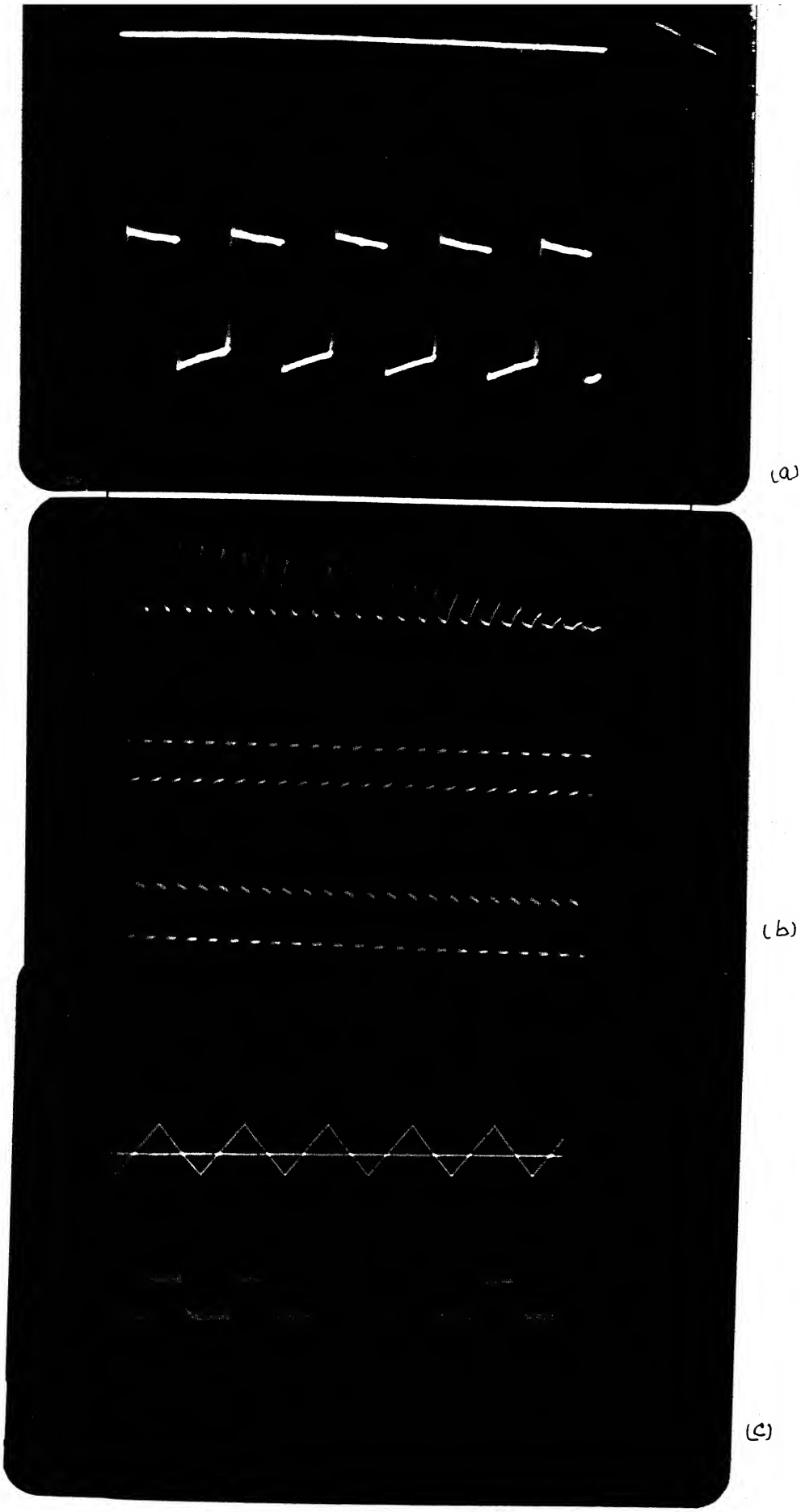

fig 6.7 Experimental oscillogram duty 0.5

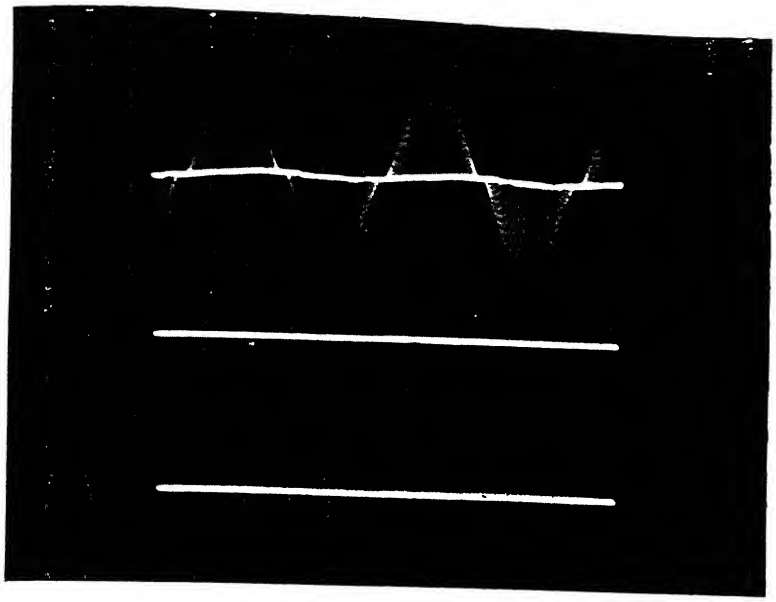

(a)

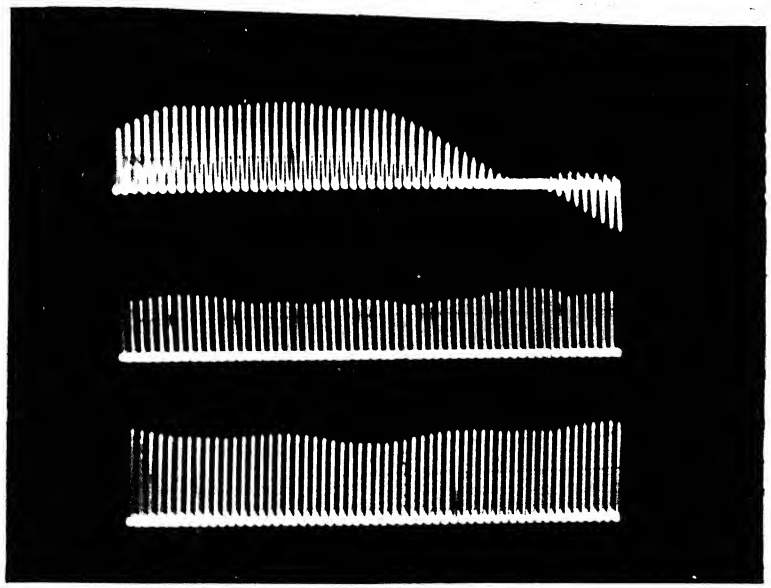

(b)

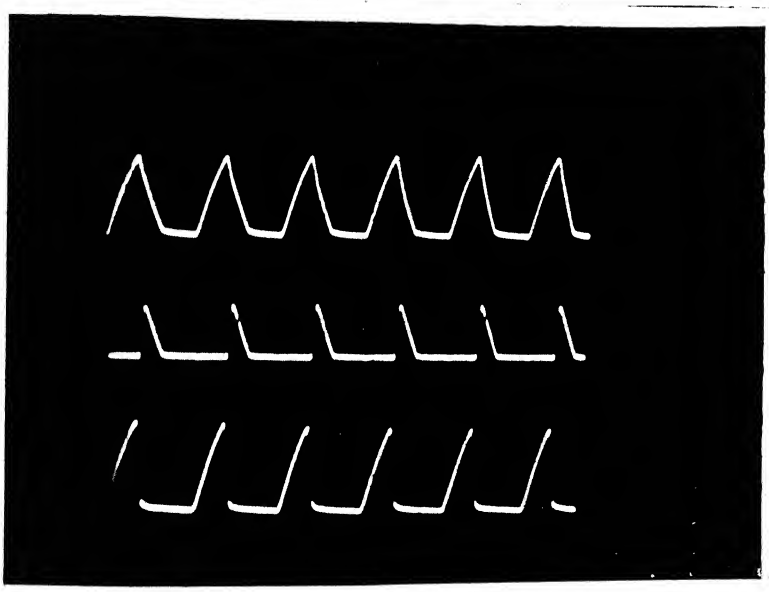

(c)

fig 6.8 Experimental oscillogram of boost inductor boost diode and boost switch duty 0.5

CHAPTER SEVEN

CONCLUSION AND FUTURE SCOPE OF WORK

Based on analysis, computer simulation and experimental study, the following conclusion are drawn :

(1) By the use of topologies shown in Fig. 1.1 - 1.4. The major limitations of conventional rectifier can be eliminated. These topologies present a resistive load to the utility grid thereby draw in phase current almost at unity power factor.

(2) The control circuit used for gate drive is simple as single boost switch is used. The power and drive circuit isolation is not necessary.

(3) There is a significant reduction in size of equipment due to reduced size of input filter. At supply frequency harmonics are reduced considerably and dominent hormonics which are at switching frequency rather than line frequency are filtered out by this filter. This feature makes the topology attractive not only for application where space and weight of equipment is main consideration, but also, in almost all applications where ac to dc conversion is used.

(4) The voltage level different from average output of the rectifier can be obtained by varying duty cycle.

(5) The ripple in output dc voltage is very low.

SCOPE OF FUTURE WORK

Since many national and international monitoring agencies are considering limits on THD, these topologies can provide most economical solution. However, since only one boost switch is used, device rating has to be higher. Therefore, there is scope to explore the possibility of operating such topologies in parallel to share the load, so that they may be utilised for commercial applications where power requirement is much higher.

Higher switching frequency results in high switching losses. The possibility of using high switching frequency in these active wave shaping circuit along with loss less snubber can be explored.

References

1. Ned Mohan, "Power electronics converters, Applications and design", John Wiley & Sons, 1994.
2. G. K. Dubey, "Power Semiconductor Controlled Drives", Prentice Hall, Englewood Cliffs, 1989.
3. G. K. Gubey, S. R. Doradla, A. Joshi and R.M.K. Sinha, "thyristorised Power Controllers", Willey Eastern Limited, 1986.
4. G.K. Dubey, "PWM Self Commutated ac to dc converters", Journal of Institute of Engineers, India, Aug. 1989, pp. 46-54.
5. V.R. Kanetkar, M.S. Dawande and G.K. Dubey, "Recent Advances in Synchronous Link Converters, IETE Book Series, Vol. 1, Power Electronics and Devices, Oct. 1993, pp. 131-151.
6. V. Vorperian and R.B. Ridley, "A Simple Scheme for Unity PF Rectification for High Frequency AC Buses", IEEE Trans. on Power Electronics, Vol. PE-5, No. 1, Jan. 1990, pp. 77-87.
7. M.S. Dawande, Switch Mode Power Rectifaction, Ph.D. Thesis, Mar. 94, I.I.T. Kanpur.
8. C.T. Pan, T.C. Chen, "Step-up / Down Three-phase AC to DC Converter with sinusoidal input current and unity power factor", IEE Proc. Electr. Power Appl., Vol. 41, No. 2, Mar. 1994, pp. 77-83.
9. A.R. Prasad, Phoivas D. Ziogas and Stepanos Manias, " Anactive power factor correction technique for three phase diode rectifiers", IEEE Transactions on Power electronics, Vol. 6, No. 1, January 1991, pp. 83-92.

10. E.H. Ismail and Robert Erickson, "Single switch 3ϕ PWM Low harmonic Rectifiers. IEEE Transaction on power electronics, Vol. 11, No. 2, March 1996, pp. 338-340.

11. Robert Martinex, Prasad N. Enjeti, "A High-performance single-phase reactifier with Input Power Factor Correction", IEEE Transaction on Power Electronics, Vol. 11, No. 2, March 1996. pp. 311-317.

12. H.L. Jou, F.C. Wu, H-Y Chu, "New Single Phase Active Power Filter", IEEE Proc-Elect., Power Appl. Vol. 141, No. 3, May 1994.

13. John W Kolar, Mans Ertl, Franz C. Zach, "A Comprehensive Design Approch for a Three-phase High-Frequency Single switch Discontinuous-Mode Boost power Factor Corrector Based on Analytically Derived Normalized Converter Component Ratings". IEEE Transactions on Industrial Applictions, Vol. 31, No. 3, May/June 1995, pp. 569-583.

14. Eugenio Wernekinck, Atsuo Kawannura, Richard Mofft, A High Frequency AC-DC Converter with unity power factor and minimum harmonic distortion, IEEE Transactions on Power Electronics, Voo. 6, No. 3, July 1991, pp. 364-370.

15. William B. Lawrance and Wladyslaw Mielezarski, "Harmonic Current Reduction in a Three-Phase Diode Bridge Rectifier, IEEE Transactions on Industrial Electronics, Vol. 39, No. 6, Dec. 1992, pp. 571-576.

16. Atluri Rama Prasad, Phoivos D. Ziogas and Stefanos Manias, "A novel Passive Waveshaping Method for Single-Phase Diode Rectifiers", IEEE Transaction on Industrial Electronics, Vol. 37, No. 6, Dec. 1990, pp. 521-530.

17. M.H. Rashid, "Power Electronics Circuit, Devices, and Applications, Prentics-Hall of India, New Delhi, 1994.

18. M.J. Kocher and R.L. Steigerwald, "An ac to dc converter with high quality input wave forms", IEEE Trans. Ind. Appl., Vol. 1A19 Nov, pp. 586-599, July / Aug. 1983.